Amphiphilic Dendrimer as Potent Antibacterial against Drug-Resistant Bacteria in Mouse Models of Human Infectious Diseases

Noah King, Dinesh Dhumal, Shi Qian Lew, Shanny Hsuan Kuo, Christina Galanakou, Myung Whan Oh, Sook Yin Chong, Nian Zhang, Leo Tsz On Lee, Zvi Hayouka, et al.

An Amphiphilic Dendrimer as Potent Antibacterial Against Drug-resistant Bacteria in Mouse Models of Human Infectious Diseases

Noah King,[1#] Dinesh Dhumal,[2#] Shi Qian Lew,[1#] Shanny Hsuan Kuo,[1] Christina Galanakou,[2] Myung Whan Oh,[1] Sook Yin Chong,[1] Nian Zhang,[3] Leo Tsz On Lee,[3,4] Zvi Hayouka,[5] Ling Peng,[2*] and Gee W. Lau[1*]

[1]Department of Pathobiology, University of Illinois at Urbana-Champaign, Urbana, IL, 61802, USA.

[2]Aix Marseille University, CNRS, Centre Interdisciplinaire de Nanoscience de Marseille (CINaM), UMR 7325, Equipe Labelisée Ligue Contre le Cancer, Parc Scientifique et Technologique de Luminy 913, 13288 Marseille, France.

[3]Faculty of Health Sciences, University of Macau, E12-3011, Taipa, Macau, China

[4]Ministry of Education Frontiers Science Center for Precision Oncology, University of Macau, Taipa, Macau, China

[5]Institute of Biochemistry, Food Science and Nutrition, The Robert H. Smith Faculty of Agriculture, Food and Environment, The Hebrew University of Jerusalem, Rehovot 76100, Israel

[#]These authors contributed equally to the paper.

*_To whom correspondence should be addressed,_ email: ling.peng@univ-amu.fr; geelau@illinois.edu

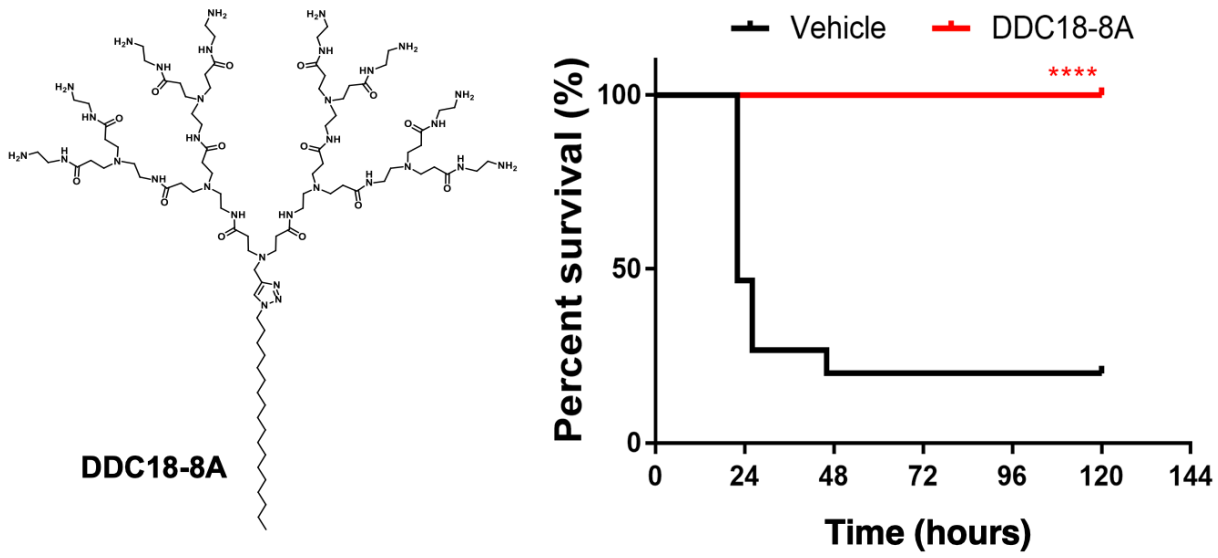

ABSTRACT

Modern medicine continues to struggle against antibiotic resistant bacterial pathogens. Among the pathogens of critical concerns are the multidrug-resistant (MDR) *Pseudomonas aeruginosa*, *Staphylococcus aureus* and *Klebsiella pneumoniae*. These pathogens are major causes of nosocomial infections among the immunocompromised individuals, involving major organs such as lung, skin, urinary tract, liver, and bloodstream. Therefore, novel approaches are direly needed. Recently, we have developed an amphiphilic dendrimer DCC18-8A exhibiting high antibacterial and antibiofilm efficacy in vitro. DCC18-8A is composed of a long hydrophobic alkyl chain and a small hydrophilic poly(amidoamine) dendron bearing amine terminals, exerting its antibacterial activity by attaching and inserting itself into bacterial membranes to trigger cell lysis. Here, we examined the pharmacokinetics, in vivo toxicity, as well as the antibacterial efficacy of DCC18-8A in mouse models of human infectious diseases. Remarkably, DCC18-8A significantly reduced the bacterial burden in mouse models of acute pneumonia and bacteremia by *Pseudomonas aeruginosa*, methicillin-resistant *Staphylococcus aureus* (MRSA) and carbapenem-resistant *Klebsiella pneumoniae*; and neutropenic soft tissue infection by *P. aeruginosa* and MRSA. Most importantly, DCC18-8A outperformed pathogen-specific antibiotics against all three pathogens by achieving similar bacterial clearance at 10-fold lower therapeutic concentrations. In addition, it showed superior stability and biodistribution in vivo, with excellent safety profiles yet without any observable abnormalities in histopathological analysis of major organs, blood serum biochemistry and hematology. Collectively, we provide strong evidence that DCC18-8A is a promising alternative to currently prescribed antibiotics in addressing challenges associated with nosocomial infections by MDR pathogens.

KEYWORDS: Amphiphilic dendrimer*, Pseudomonas aeruginosa, Staphylococcus aureus, Klebsiella pneumoniae, in vivo efficacy.*

A serious threat for human and animal health is the ongoing arms race between the development of new antibiotics and the emergence of antibiotic-resistant (ABR) bacteria. The United States Center for Disease Control (U.S. CDC) estimated that in 2019,[1] there were more than 2.8 million antibiotic-resistant infections, with greater than 35,000 mortalities.[2] Current annual mortality associated with antibiotic resistance is greater than 700,000 people globally. Although antibiotics are the most commonly used method for treating bacterial infections, they have also driven the emergence of multidrug-resistant (MDR), extensively drug-resistant (XDR) and pandrug-resistant (PDR) bacteria.[3] Apart from poor antimicrobial stewardship, recent studies in microbial ecology have given rise to the notion of the antibiotic resistome, where both pathogenic and nonpathogenic bacteria within the environment harbor a reservoir of all antibiotic resistance genes and their precursors, are constantly being bombarded by different chemicals. Consequently, bacteria have developed mechanisms to defend themselves against other microbes and toxic chemicals, leading to the evolution of highly specific resistance elements even in the absence of innate antibiotic production.[4-5]

Among bacterial pathogens, the ESKAPEE pathogens (*Enterococcus faecium, Staphylococcus aureus (including methicillin-resistant S. aureus MRSA), Klebsiella pneumoniae, Acinetobacter baumannii, Pseudomonas aeruginosa, Enterobacter* species, and *Escherichia coli*) are highly recalcitrant to antibiotics, while being major causes of human infectious diseases, especially in nosocomial settings. *P. aeruginosa* is an opportunistic pathogen that causes numerous infections varying from local to systemic, and from benign to life-threatening. *P. aeruginosa*-mediated pneumonia and pneumonia-derived sepsis, particularly of ventilated patients in intensive care units, are associated with high morbidity and mortality.[6-7] Additionally, *P. aeruginosa* is one of the dominant pathogens in patients with a variety of chronic lung diseases, including cystic fibrosis, advanced chronic obstructive pulmonary disease, primary ciliary dyskinesis and bronchiectasis. [8-9] *P. aeruginosa* is also the dominant pathogen in chronic suppurative otitis media,[10] severe ocular infection,[11-12] and burn sepsis.[13] *S. aureus, including the methicillin-resistant (MRSA)* strains, are opportunistic asymptomatic colonizers, with one in three humans carrying the bacterium in their nose without any illness, but can cause serious infection in immunocompromised individuals. *S. aureus* is one of the five most common causes of hospital-acquired infections, ranging from minor skin infections and abscess formation,[14] to life-threatening diseases such as acute pneumonia, chronic pneumonia, endocarditis, toxic shock syndrome and bacteremia/sepsis,[6-7] which are difficult to treat. *K. pneumoniae* is one of the few Gram-negative opportunistic pathogens widely known to cause primary pneumonia,[15] and is a leading cause of nosocomial pneumonia,[16] but also the most frequent causes of urinary tract infections and bacteremia in immunocompromised individuals.[16] Especially, the hypermucoviscous, hypervirulent KP (hvKp) strains account for 12 to 45% of *KP* cases in endemic areas,[17] are capable of causing community-acquired and, increasingly, hospital-acquired infections, and often infect otherwise healthy individuals.[18-19] Therefore, non-antibiotic alternatives are urgently needed to effectively treat infectious diseases mediated by these pathogens.

An alternative class of antibacterials are the amphiphilic antimicrobial peptides (AMPs) comprised of cationic surface charges and hydrophobic components.[20-22] Positively-charged amino acid residues on AMPs interact electrostatically with the negatively-charged bacterial surface, followed by penetration of their hydrophobic entity into the bacteria cell membrane to cause membrane disruption and cell lysis.[20-22] It is to note that amphiphilic dendrimers are emerging to mimic AMPs for promoting antibacterial activity while preventing resistance development.[23-27] The amphiphilic dendrimers are composed of distinct hydrophobic components and hydrophilic dendritic structures bearing cationic terminals, with intrinsic feature to mimic AMPs for antibacterial potential. Also, their unique dendritic architecture, comprising a central core, branch units and terminal functional groups, creates steric hindrance hence inherent stability against enzymatic degradation.[28-29] In addition, the amphipathic nature of these dendrimers allows them to self-assemble into nanostructures, facilitating their interaction with bacteria via multivalent interactions for more effective antibacterial activity.[24, 27]

We have recently developed an amphiphilic dendrimer (DCC18-8A) composed of a long hydrophobic alkyl chain and a small hydrophilic poly(amidoamine) dendron bearing amine terminals (Figure 1),[27] which efficiently killed both Gram-positive and Gram-negative pathogens, including drug-resistant bacteria *in vitro*, and prevented biofilm formation without overt cytotoxicity toward cultured kidney and fibroblast cells. However, its efficacy against pathogenic bacteria have not been examined *in vivo*. Here, we investigated the efficacy DCC18-8A against three ESKAPE pathogens, *P. aeruginosa*, MRSA, and *K. pneumoniae* in mouse models of acute pneumonia, bacteremia and neutropenic soft tissue infection, as well as its toxicity and pharmacokinetics properties in mice.

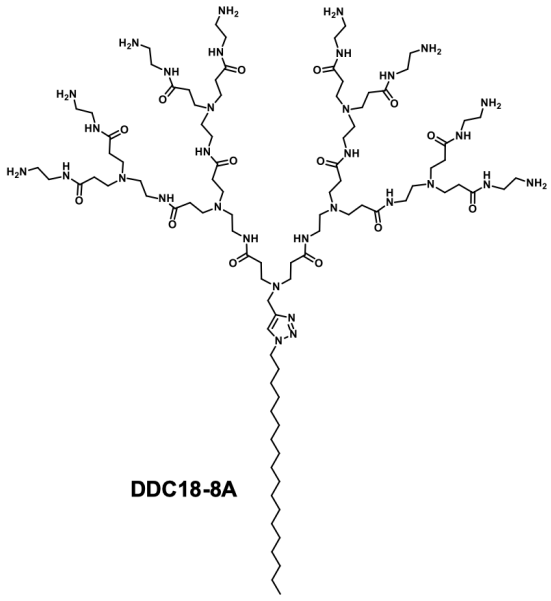

Figure 1. Structure of the dendrimer DDC18-8A.

DCC18-8A is a broad spectrum antibacterial that does not induce resistance

We examined the minimum inhibitory concentrations (MICs) of DCC18-8A, and found that the dendrimer efficiently killed multiple Gram-positive and Gram-negative bacteria cultured statically in LB (Table 1). However, the killing of *K. pneumoniae* appeared to be strain dependent with BAA-1705 susceptible but ATCC 13883 and ATCC 2146 resistant to the killing by DCC18-8A (Table 1).

Table 1. In vitro minimal inhibitory concentration (MIC)* against different bacterial strains.

Organisms	**MIC (μg/mL)**
Gram-positive bacteria	
Staphylococcus aureus USA300LAC (MRSA)	24
Staphylococcus aureus ATCC 25904	12
Staphylococcus aureus ATCC 43300 (MRSA)	12
Bacillus subtilis strain 168 (ATCC 23857)	3
Gram-negative bacteria	
Escherichia coli MG1655	6
Escherichia coli Y8 (multidrug-resistant)	6
Acinetobacter baumannii ATCC 17978	6
Acinetobacter baumannii ATCC 1791 (multidrug-resistant)	6
Klebsiella pneumoniae BAA-1705	24
Klebsiella pneumoniae ATCC 13883	> 96
Klebsiella pneumoniae ATCC 2146 (multidrug-resistant)	> 96
Pseudomonas aeruginosa PAO1	12
Pseudomonas aeruginosa PAK	12
Citrobacter rodentium DBS100	6
Salmonella enteritidis ATCC 13076	6
Vibrio parahaemolyticus RIMD 2210633	6
Vibrio alginolyticus ATCC33787	6

*MIC was determined by using the lysogeny broth (LB) as described in the Methods.

Next, we assessed the efficacy of DDC18-8A in both time and dose-dependent killing of *P. aeruginosa* strain PA01, MRSA strain USA300LAC, and *K. pneumoniae* strain BAA-1705. These strains are virulent in various preclinical mouse models of human infectious disease, including acute pneumonia, bacteremia, immunosuppressed soft tissue infection, and sepsis.[30-32] Overnight culture of these strains were serial diluted to10^7-10^8 colony forming units (CFU) and treated DDC18-8A, with phosphate-buffered saline (PBS) and bacterial-specific antibiotics served as the controls. DDC18-8A effectively killed PA01, USA300LAC, and BAA-1705, all in a concentration- and time-dependent manner (Figure 2A-C). DDC18-8A displayed comparable efficacy to tobramycin and daptomycin against *P. aeruginosa* strain PA01 and MRSA USA300LAC, respectively. *K. pneumoniae* BAA-1705 was efficiently killed by DDC18-8A but not Tigecycline, which was bacteriostatic. The minimum bactericidal concentrations (MBCs) of DCC18-8A against these strains are listed in Table S1. For additional comparison, previous *in vitro* studies have shown that tobramycin,[33] vancomycin,[34] and imipenem[35] reduced the viable count of selective antibiotic resistant strains of *P. aeruginosa*, MRSA, and *K. pneumoniae* by 2 logs, 5 logs, and 2 logs, respectively. These results confirm that DDC18-8A is indeed highly potent against both Gram-positive and Gram-negative bacterial pathogens.

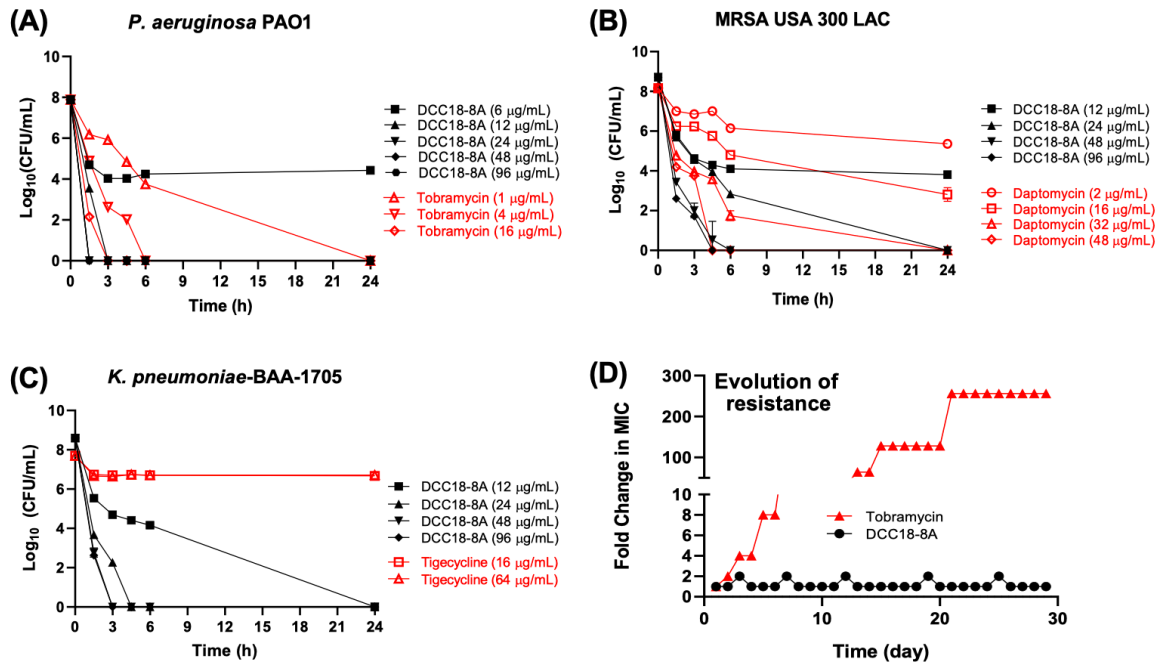

Figure 2. *In vitro* killing and evolution of resistance. (A-C) *P. aeruginosa* strain PAO1, MRSA strain USA300LAC, and *K. pneumoniae* strain BAA-1705 were exposed to indicated concentration of DCC18-8A, sterile PBS or antibiotics for the specified duration in PBS while rotating at 37° C. before serially dilution plating onto lysogeny agar plates for CFU determination. Data represent mean ± SD (n = 3 per group). (D) Resistance development after 30 days of serial passaging in LB with the initial 0.25 – 4.0 x MIC concentrations of DCC18-8A (3 - 48 μg mL^{-}) or tobramycin (0.25 - 4 μg mL^{-}).

As mentioned previously, antibiotic resistance is rampant among *P. aeruginosa*, *S. aureus*, *K. pneumoniae*, which serves a major driver of their success as nosocomial pathogens. An ideal antibacterial will be one which is resistance to the emergence of resistance. We compared the experimental evolution of resistance by serial passaging *P. aeruginosa* strain PA01 in 0.25–4.0 × MIC concentrations DDC18-8A versus tobramycin for 30 days. No discernable resistance to DDC18-8A was observed in PAO1. In contrast, the resistance to tobramycin increased by 256-fold within the 30-day duration (**Fig. 2D**). These results indicate that DDC18-8A offers greater potential in resisting the development of resistance.

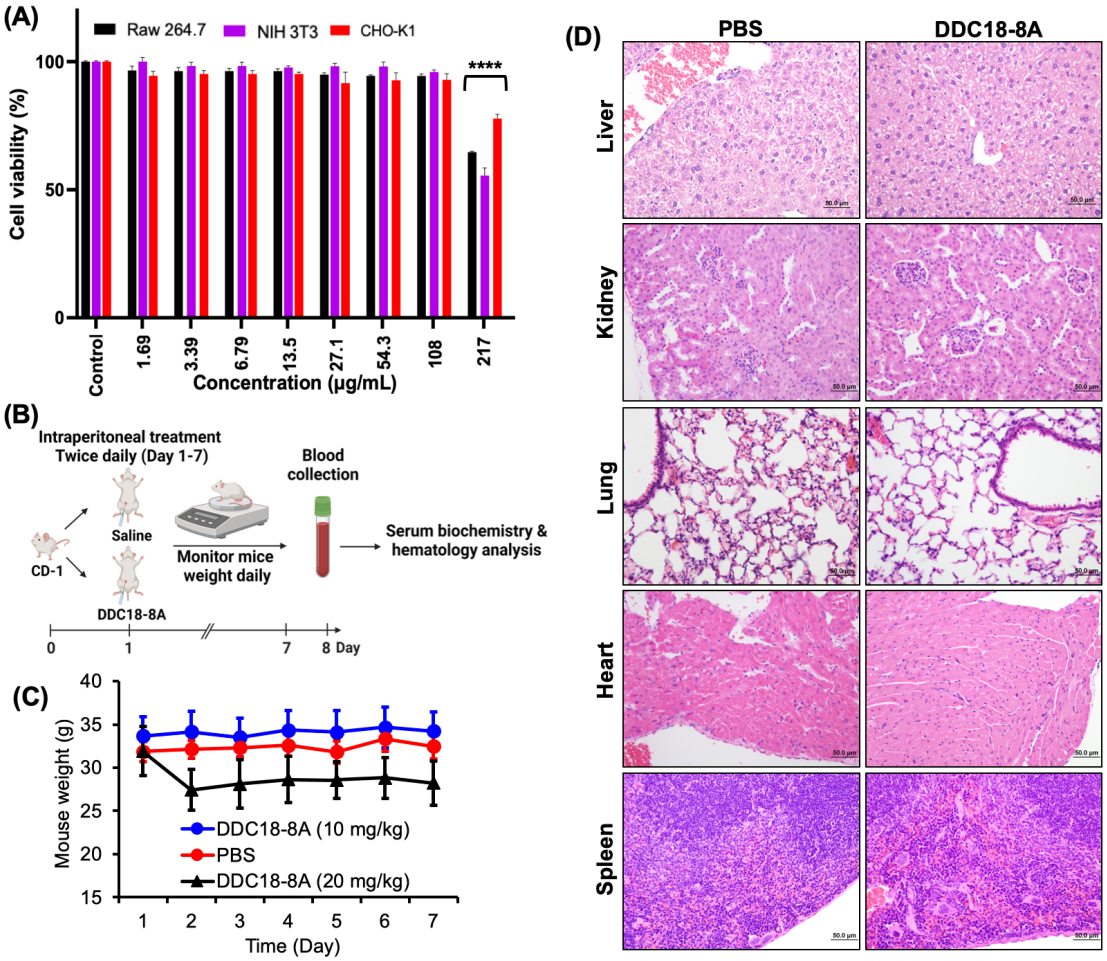

Figure 3. Toxicity profiles of DDC18-8A. (A) Viability of cultured RAW264.7, NIH3T3 and CHO-K1 cells after 24 hours of exposure to indicated concentrations of DDC18-8a, as determined by the Presto Blue cell viability assay. Error bars represent SEM for n=3. **** $p < 0.0001$ compared to vehicle with the Student's t-test. (B-C) Experimental scheme and mouse weight of CD-1 mice after 7 days of intraperitoneal injection with DDC18-8A (5 mg/kg, twice daily; 20 mg/kg, once daily). Error bars represent SD for n=5. (D) Representative H&E stained histopathological images of livers, kidneys, lungs, hearts, and spleens from mice in (B). Magnification: 400X.

DDC18-8A has excellent safety profiles

Prior to determining whether DDC18-8A would be efficacious in animal models of human infectious diseases, we examined its cytotoxicity and in vivo toxicity. DDC18-8A was non-cytotoxic between 1.69 μg/mL -108 μg/ml against multiple cultured immortalized cell lines, including the mouse macrophage RAW264.7, mouse fibroblast NIH3T3 cells, and a derivative of the Chinese hamster ovary CHO cell line CHO-K1 (Figure 3A). Even though DDC18-8A was moderately cytotoxic to all three cell lines at 217 μg/ml, it should be noted that this approximates 22-fold higher than our current therapeutic concentration of 5 mg/kg twice daily dose used in animal models (see below). These results indicate that DDC18-8A is unlikely to be cytotoxic at therapeutic concentrations.

Next, we investigated the toxicity potential of DDC18-8A in mice. Seven–week old CD-1 mice (groups of 5) were intraperitoneally-inoculated with 5.0 mg/kg of DDC18-8A twice daily for seven days, with the control group challenged with same volume of sterile PBS. DDC18-8A did not alter the mouse weights within the 7-day duration (Figure 3B-C). Moreover, we examined the tolerated dose in more detail, and found that once daily intraperitoneal injection of DDC18-8A at 20 mg/kg caused approximately 10-15% weight loss in mice (Figure 3C, Day 2, 14.1%; Day 3, 12.0%; Day 4, 10.3%; Day 5, 10.5%; Day 6, 9.8%; Day 7, 11.7%), suggesting that an acceptable therapeutic dose of DDC18-8A can reach up to 20 mg/kg.

Importantly, there was no overt evidence of treatment-associated toxicity or inflammatory changes in the histopathology of livers, kidneys, lungs, hearts and spleens between the PBS versus the DDC18-8A treated mice at 5.0 mg/kg twice daily, except for the hepatocytes were multifocally and mildly laden with intracytoplasmic clear vacuoles in both the control group and DDC18-8A group (Figure 3D). The cytoplasmic vacuolation in liver is non-specific and often occurs as consequence of physiological glycogen infiltration after feeding.

For serum biochemistry, a few insignificant findings are revealed in both the saline and DDC18-8A groups, including a mild degree of hyperbilirubinemia, hypocalcemia and hyperglobulinemia (Table 2). The predominant causes of conjugated hyperbilirubinemia are intrahepatic cholestasis and extrahepatic obstruction of the biliary tract. However, there are normal levels of alkaline phosphatase (ALP, marker of hepatocellular damage) and alanine transaminase (ALT, marker of cholestasis) in both cohorts, indicating no abnormality in liver function and biliary drainage. This concern is also mitigated by the fact that both vehicle and DDC18-8A-treated mice have normal levels of albumin (indicator of proper hepatic synthetic function with no signs of liver insufficiency) and unremarkable liver histopathology, which all refute an underlying liver dysfunction. The likely cause of hyperbilirubinemia in this case could be hemolysis during blood collection, which would have increased bilirubin levels artifactually. The likely cause of hypocalcemia was due to the use of heparin sulfate as anticoagulant for blood collection. Excessive heparin chelates calcium in blood samples, often gives false appearance of hypocalcemia. Similar issue is also found in another commonly used anticoagulant EDTA, which will also completely or partially chelate calcium and result in low calcium values. Common causes of hyperglobulinemia include hemoconcentration (dehydration), inflammation, and paraproteinemia from B-lymphocyte neoplasia. The

normal A:G (albumin/globulin ratio) in most mouse species approximates 1:1. High total protein with a normal A:G ratio would suggest dehydration (non-selective hyperglobulinemia), while the same protein with a low A:G ratio (<1) would indicate true hyperglobulinemia (selective hyperglobulinemia). In our study on DDC18-8A, the A:G (albumin/globulin ratio) is closer to 1, which more likely suggests a nonselective hyperglobulinemia that is likely secondary to dehydration.

Table 2. Blood chemistry of CD-1 mice after exposure to DDC18-8A

Analyte	Saline	DDC18-8A	Reference range*
Creatinine	0.15 ± 0.062	0.12 ± 0.05	0.1-0.4
BUN (urea)	24.67 ± 3.51	21.75 ± 2.99	16-29
Total protein	6.10 ± 0.62	6.08 ± 1.19	5.0-6.3
Albumin	3.47 ± 0.45	3.42 ± 0.81	3.0-4.1
Globulin	2.63 ± 0.21	2.65 ± 0.39	1.8-2.3
Albumin/globulin ratio	1.33 ± 0.06	1.30 ± 0.12	1.3-2.0
Calcium	7.93 ± 1.16	7.80 ± 1.12	9.8-10.8
Phosphorus	8.07 ± 0.32	8.85 ± 0.98	6.1-13.1
Sodium	147.00 ± 6.08	147.50 ± 7.85	147.9-155.2
Potassium	8.93 ± 1.76	9.78 ± 6.00	8.3-12.7
Sodium/potassium ratio	17.00 ± 4.00	19.75 ± 10.50	
Chloride	108.00 ± 2.31	106.50 ± 3.32	106.1-113.1
Glucose	110.33 ± 21.59	178.00 ± 39.82	147-361
Alkaline phos total	51.50 ± 26.50	56.50 ± 2.50	34-106
ALT (SGPT)	52.00 ± 3.27	47.67 ± 14.61	25-76
GGT	QNS	QNS	36-89
Total bilirubin	1.30 ± 0.46	1.45 ± 1.32	0.16-0.31
Cholesterol total	225.00 ± 44.58	229.25 ± 85.90	168-275
Triglycerides	163.00 ± 38.97	123.75 ± 12.04	51-161
Bicarbonate (TCO2)	12.00 ± 2.00	14.25 ± 1.26	N/A
Anion gap	36.50 ± 2.50	34.75 ± 2.22	N/A
Hemolytic indicator	4.00 ± 0.00	4.00 ± 0.00`	N/A

*Reference range was according to the values found in the Reference 74, as well as from the technical sheet provided by the Charles River Laboratories.

For hematology, slightly lower hematocrit levels are noted in both the saline and DDC18-8A groups with other RBC-related parameters (i.e. RBC count, hemoglobin, mean cell volume, MCH, MCHC) within normal limits. Hence, such findings are likely physiologically insignificant. Low platelet counts are revealed in both mouse groups, most likely due to the blood clotting during the sample collection process (Table 3). Collectively, our extensive in vitro and in vivo analyses indicate that DDC18-8A has excellent safety profiles and will be amendable for examining efficacy against bacterial infection in vivo.

Table 3. Complete blood count with differential of CD-1 mice after exposure to DDC18-8A.

Analyte	Saline	DDC18-8A	Reference range*
Red blood cells ($x10^6/mL$)	8.04 ± 1.03	8.33 ± 0.75	7.31-12.27
Hemoglobin (g/dL)	13.30 ± 1.30	13.8 ± 0.37	11.9-18.4
Hematocrit (%)	37.73 ± 4.03	39.50 ± 2.85	39.7-74.7
Mean cell volume (fL)	47.00 ± 1.21	47.33 ± 1.93	46.5-69.0
MCH (pg)	16.60 ± 1.18	16.68 ± 1.50	13.1-18.1
MCHC (g/dL)	35.30 ± 1.75	35.08 ± 2.41	35.1-38.5
Platelet estimate ($x10^3/mL$)	715.33 ± 223.99	800.00± 227.57	926.0-1539.0
WBC count ($x10^3/mL$)	3.36 ± 1.59	5.89 ± 1.11	4.44-14.01
Neu (%)	13.90 ± 11.94	9.65 ± 7.74	8.74-55.68
Lymph (%)	81.90 ± 16.81	86.85 ± 3.42	37.50-85.01
Mono (%)	2.13 ± 2.20	2.65 ± 1.70	2.84-13.09
Eos (%)	1.93 ± 0.12	0.80 ± 0.98	0.30-5.20
Baso (%)	0.13 ± 0.23	0.05 ± 0.10	0.01-1.70
A Neu ($x10^3/mL$)	0.39 ± 0.25	0.56 ± 0.11	0.53-5.17
A Lymph ($x10^3/mL$)	2.83 ± 1.63	5.12 ± 1.00	2.06-10.01
A Mono ($x10^3/mL$)	0.067 ± 0.058	0.165 ± 0.13	0.18-1.32
A Eos ($x10^3/mL$)	0.063 ± 0.032	0.048 ± 0.062	0.01-0.83
A Baso ($x10^3/mL$)	0.0033 ± 0.0058	0.00 ± 0.00	0.00-0.17

*Reference range was according to the values as published in Reference 74, as well as from the technical sheet provided by the Charles River Laboratories.

DDC18-8A displays high stability and excellent biodistribution in vivo

We examined biostability and biodistribution of the intraperitoneally-administered Cyanine7.5 conjugated-DDC18-8A (Cy7.5/DDC18-8A) spatiotemporally over 72 hours by using an IVIS Spectrum CT imaging system in the absence of bacterial challenge (Figure 4A, B) as well as during a MRSA-mediated acute pneumonia (Figure 4C-E). Importantly, intraperitoneally-injected Cy7.5/DDC18-8A exhibited high stability and favorable biodistribution and continued to circulate well beyond 72 hours post injection when administered alone or for the duration of the MRSA acute pneumonia (24 hours), with the fluorescence signals accumulate in all major organs, including in the MRSA-infected mouse lungs. However, more detailed analysis are needed to determine whether there was accumulation in the infected lungs via the enhanced permeability and retention (EPR) effect[36] mediated by potentially leaky vasculature and dysfunctional lymphatic drainage in these infected tissues.[37-38] The high stability of DDC18-8A indicate that it could be resistant to degradation by host and bacterial proteases. Therefore, DDC18-8A is able to overcome the disadvantages of some AMPs which are proteolytically unstable with short half-lives that lower their antimicrobial potency in vivo. Also, it should be noted that due to the loss of blood during organs harvesting, the fluorescence signals, particularly in the hearts, were artificially lower. Additionally, uptake of DDC18-8A in brain was observed (Figure 4B), highlighting that DDC18-8A was able to cross the blood-brain barrier and accumulate in the brain, hence having potential therapeutic use

in cases of bacterial meningitis. However, because of its the amphipathic nature, DDC18-18A may intercalate into the alveolar surfactant layer and disrupt the airspace patency, resulting in respiratory distress, and hence, unsuitable for direct administration into the lung at the current therapeutic concentration. Finally, the minor changes in the fluorescence signal intensity of each mouse in different time points was likely caused by different positioning of mouse abdomen relative to the camera (Figure 4D).

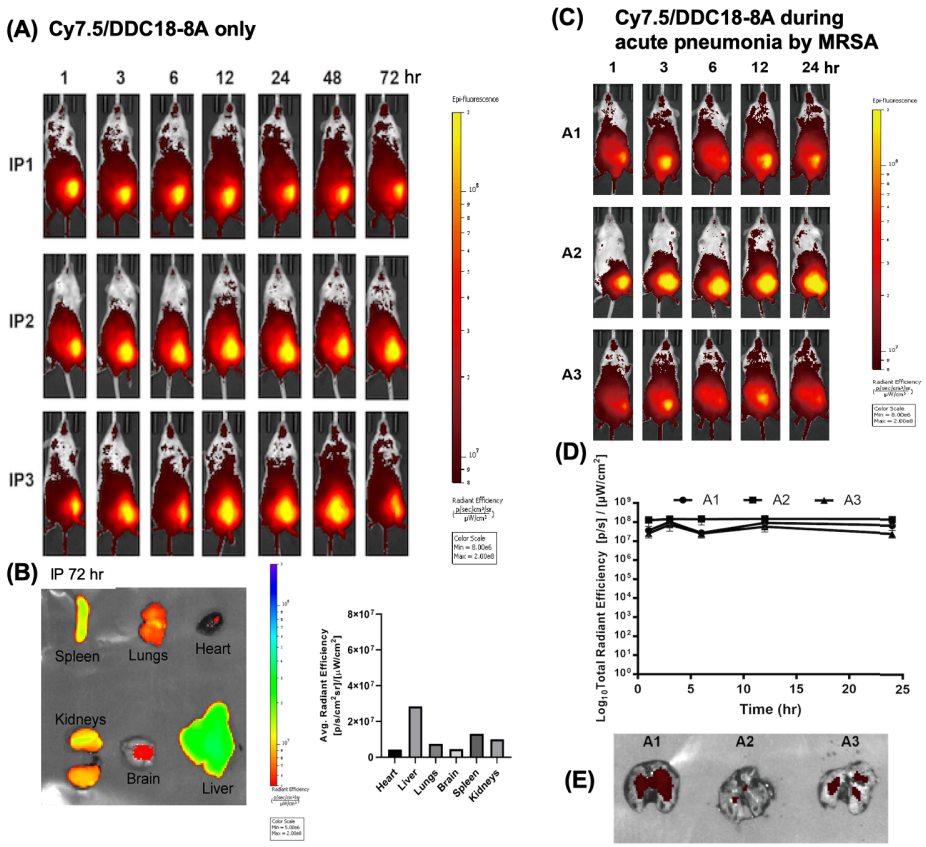

Figure 4. Pharmacokinetic properties of DDC18-8A. (A) Biostability and biodistribution of intraperitoneally-injected Cy7.5/DDC18-8A (1.67 mg/kg) over 72 hours in CD-1 mice (n=3) and imaged by an IVIS SpectrumCT imager. (B) Major organs were excised from a typical mouse at 72-hour post administration, imaged in a rainbow color scale, and quantified. (C) Pharmacokinetics of Cy7.5/DDC18-8A (1.67 mg/kg) during MRSA USA300LAC-mediated acute pneumonia. Cy7.5/DDC18-8A was injected intraperitoneally immediately after intranasal inoculation of 1.08 x 10^8 CFU of MRSA USA300LAC into CD-1 mice (n=3), and imaged with an IVIS SpectrumCT Imager for the duration of 24-h infection. (D) Quantification of mouse signals in (C) by the Living Image® Software (PerkinElmer). (E) Lungs from C were harvested at 24-h and imaged.

DDC18-8A is efficacious against acute pneumonia infection by bacterial pathogens

P. aeruginosa, *S. aureus* including MRSA, and *K. pneumoniae* are major causes of pulmonary infection as well as bacteremia and sepsis, especially those acquired in hospital setting.[6-9, 13, 15-16] We examined the efficacy of DDC18-8A against acute pneumonia infection mediated by *P. aeruginosa* strain PAO1, MRSA strain USA300LAC, and *K. pneumoniae* strain BAA1705 (Figure 5A). When compared against the

vehicle control, intraperitoneally-administered DDC18-8A effectively reduced the bacterial burden in the infected lungs of CD-1 mice of PAO1, USA300LAC and BAA1705 by 5.05, 2.69 and 1.81 log, respectively (Figure 5B). The extent of bacterial load attenuation was comparable to those mediated by tobramycin (4.63), daptomycin, (2.04) and tigecycline (2.43), respectively (Figure 5B). These results suggest that the amount of accumulated DDC18-8A in the mouse lungs was adequate to exert its antibacterial effects without potential disruption to the alveolar surfactant layer. It is important to note that the dose used for DDC18-8A was only 5.0 mg/kg, which is 1/10 of those used for antibiotic treatment (50 mg/kg). This highlights the superior potential of DDC18-8A in treating acute pulmonary infection in mouse models.

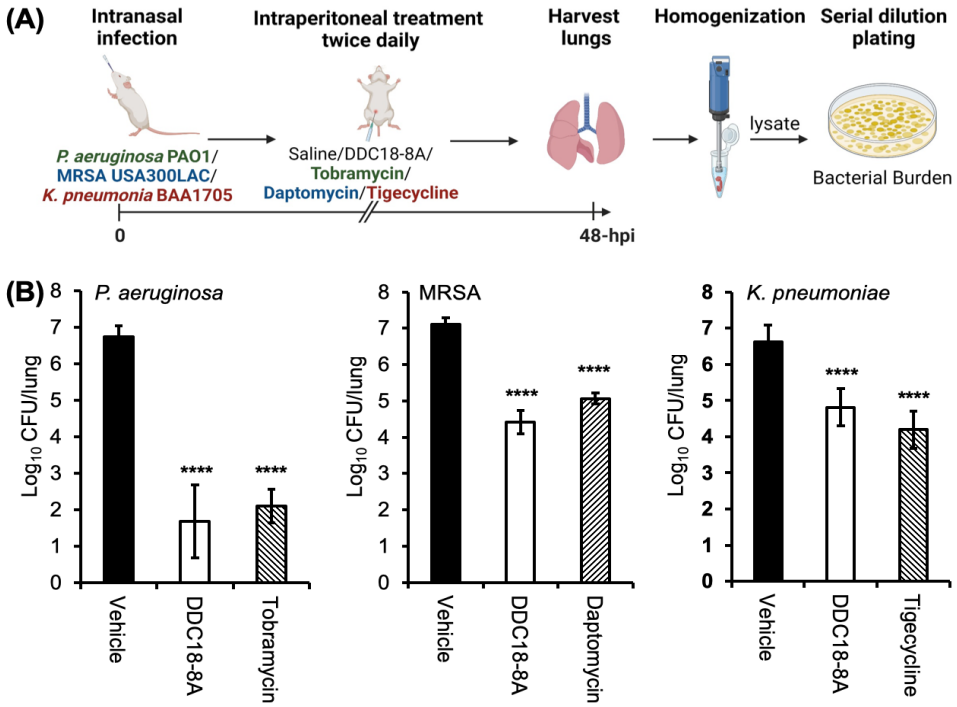

Figure 5. Efficacy of DDC18-8A in acute pneumonia against bacterial pathogens. (A) Experimental scheme. CD-1 mice (groups of 8, males and females, 7–week old) were intranasally-infected with 3.8 x 10^7 CFU of *P. aeruginosa* strain PAO1, 3.8 x 10^8 CFU of MRSA USA300LAC, and 8.1 x 10^8 CFU of *K. pneumoniae* strain BAA1705, respectively. Mice were treated with DDC18-8A (IP, 5 mg kg^{-1}, twice daily), bacterial-specific antibiotic (PA01, tobramycin IP, 50 mg kg^{-1}, once daily; USA300LAC- daptomycin SQ, 50 mg kg^{-1}, once daily; BAA1705- tigecycline IP, 50 mg kg^{-1}, once daily), or an equal volume of vehicle (sterile water). (B) Bacterial burden was determined at 48-hpi from infected lungs. Error bars represent SD for n=8. ****p < 0.0001 significance compared to vehicle control as determined by the Student's t-test.

DDC18-8A is efficacious against bacteremia infection

Next, we investigated efficacy of DDC18-8A against bacteremia infection in mice initiated by intraperitoneal injection of *P. aeruginosa* strain PAO1, MRSA strain USA300LAC, and *K. pneumoniae* strain BAA1705 (Figure 6A). When compared against the vehicle control, DDC18-8A effectively reduced the systemic bacterial burden in the infected spleens, kidneys, hearts, lungs and livers of CD-1 mice of PAO1 by 2.99, 3.39, 2.81, 2.94, and 3.21 log, respectively. Similarly, DDC18-8A effectively reduced the

systemic burden of USA300LAC-infected spleens, kidneys, hearts, lungs and livers by 3.60, 3.23, 2.49, 3.62, and 3.77 logs, respectively. Finally, DDC18-8A reduced the burden of BAA1705-infected spleens by 3.52 logs (Figure 6B). In each case, the levels of attenuation achieved by DDC18-8A was similar if not better than those attained by pathogen-specific antibiotics. Also, the dose used for DDC18-8A treatment (5.0 mg/kg) is 10-fold less than that of antibiotic treatment (50 mg/kg). Collectively, these results suggest that DDC18-8A is highly efficacious in attenuating disseminating bacterial infection mediated by the aforementioned ESKAPE pathogens.

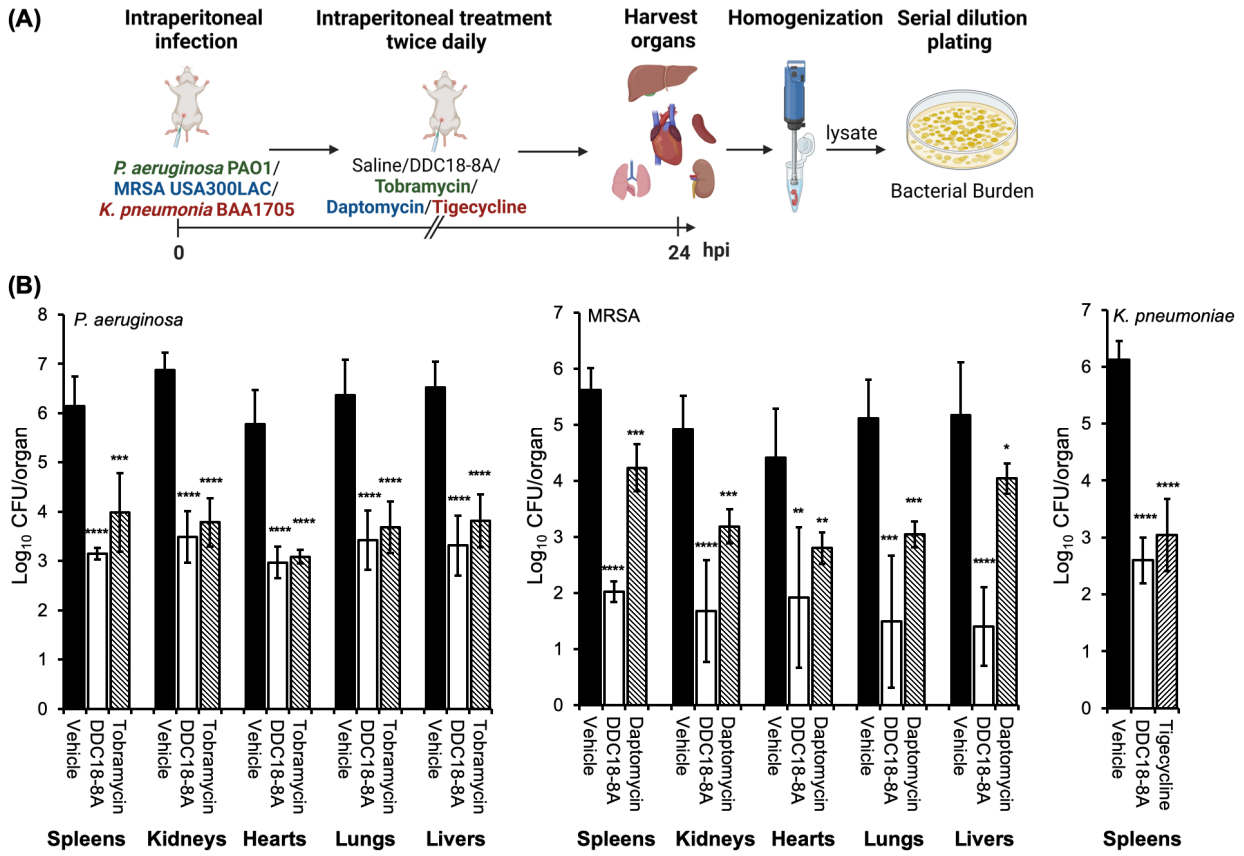

Figure 6. Efficacy of DDC18-8A against bacteremia. (A) Experimental scheme. CD-1 mice (groups of 6, males and females, 7–week old) were intraperitoneally-infected with 1.14 x 10^7 CFU of *P. aeruginosa* strain PAO1, 1.08 x 10^8 CFU of MRSA USA300LAC, and 8 x 10^6 CFU of *K. pneumoniae* strain BAA1705, respectively. Mice were treated with DDC18-8A (IP, 5 mg kg^{-1}, twice daily), bacterial-specific antibiotic (PA01, tobramycin IP, 50 mg kg^{-1}, once daily; USA300LAC- daptomycin SQ, 50 mg kg^{-1}, once daily; BAA1705- tigecycline IP, 50 mg kg^{-1}, once daily), or an equal volume of vehicle (sterile water). (B) Bacterial burden was determined at 24-hpi from infected spleens, kidneys, hearts, lungs and livers. Error bars represent SD for n=6. *p < 0.05, **p < 0.01, ***p < 0.001 ****p < 0.0001 significance compared to vehicle control as determined by the Student's t-test.

DDC18-8A is efficacious against soft tissue infection in immunosuppressed mice

The immunosuppressed neutropenic soft tissue thigh infection is frequently utilized to assess the efficacy of experimental antibacterials because of minimal interference from host neutrophil-mediated pathogen

clearance.[32, 39-41] Mice were rendered neutropenic by injection of cyclophosphamide before thigh infection with *P. aeruginosa* PAO1 and MRSA USA300LAC (Figure 7A). When compared against the vehicle control groups, DDC18-8A at the dose of 5.0 mg/kg twice daily attenuated the thigh burden of PAO1 and USA300LAC by 4.17 and 4.47 log, respectively. The levels of attenuation were comparable to those achieved by tobramycin (4.88 log) and daptomycin (4.95 log) at the doses of 50 mg/kg, respectively (Figure 7B, C). These results indicate that DDC18-8A is effective in controlling bacterial infection in the immunocompromised hosts.

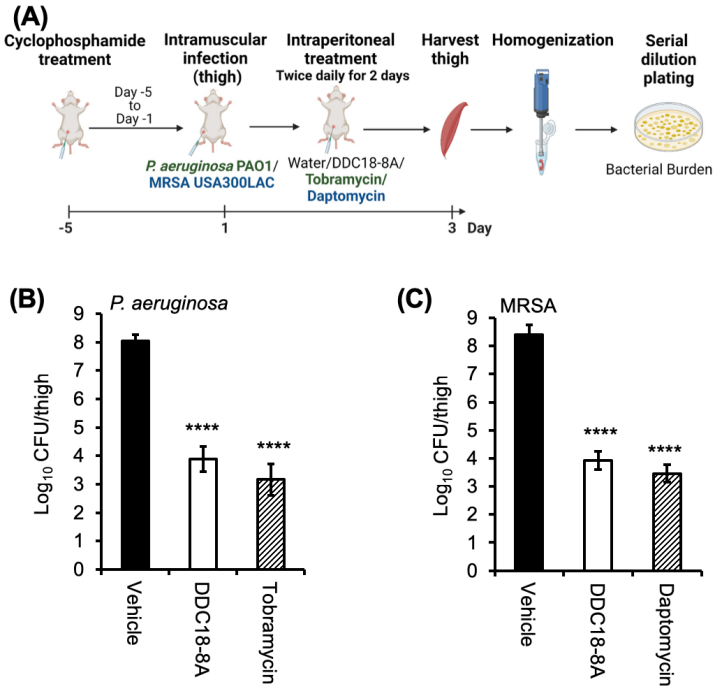

Figure 7. Efficacy of DDC18-8A against bacterial pathogens in immunosuppressed hosts. (A) Experimental scheme of neutropenic soft tissue infection. Thighs of CD-1 mice pretreated with cyclophosphamide (groups of 6, males and females, 7–week old) were intramuscularly-injected with 5.2 x 10^5 CFU of *P. aeruginosa* strain PAO1, and 1.6 x 10^6 CFU of MRSA USA300LAC (in 25 µl), respectively. Mice were treated with DDC18-8A (IP, 5 mg kg^{-1}, twice daily), bacterial specific antibiotic (PA01, tobramycin IP, 50 mg kg^{-1}, once daily; USA300LAC-daptomycin SQ, 50 mg kg^{-1}), or an equal volume of vehicle (sterile water). (B, C) Bacterial burdens were determined at 48-hpi from infected thighs. Error bars represent SD for n=6. ****p < 0.0001 significance compared to vehicle control as determined by the Student's t-test.

DDC18-8A improves mouse survival in lethal bacteremia challenge and dampens proinflammatory response-mediated by LPS aggregates

Because *P. aeruginosa* is a major cause of sepsis in humans, we examined whether DDC18-8A could meet the stringent criterium of improving mouse survival in a model of lethal bacteremia challenge by *P. aeruginosa* PAO1 (Figure 8A). CD1 mice (cohorts of 15) were intraperitoneally-infected with PAO1 bacteria and treated twice daily with 5.0 mg/kg of intraperitoneally-administered DDC18-8A. The vehicle mouse group was treated with the same volume of sterile H_2O. Infected mice treated with PBS exhibited

80% mortality rate within 120 h post-infection. In contrast, infected mice treated with DDC18-8A exhibited 100% survival rate (Figure 8B), highlighting the therapeutic potential of DDC18-8A in attenuating bacterial infections.

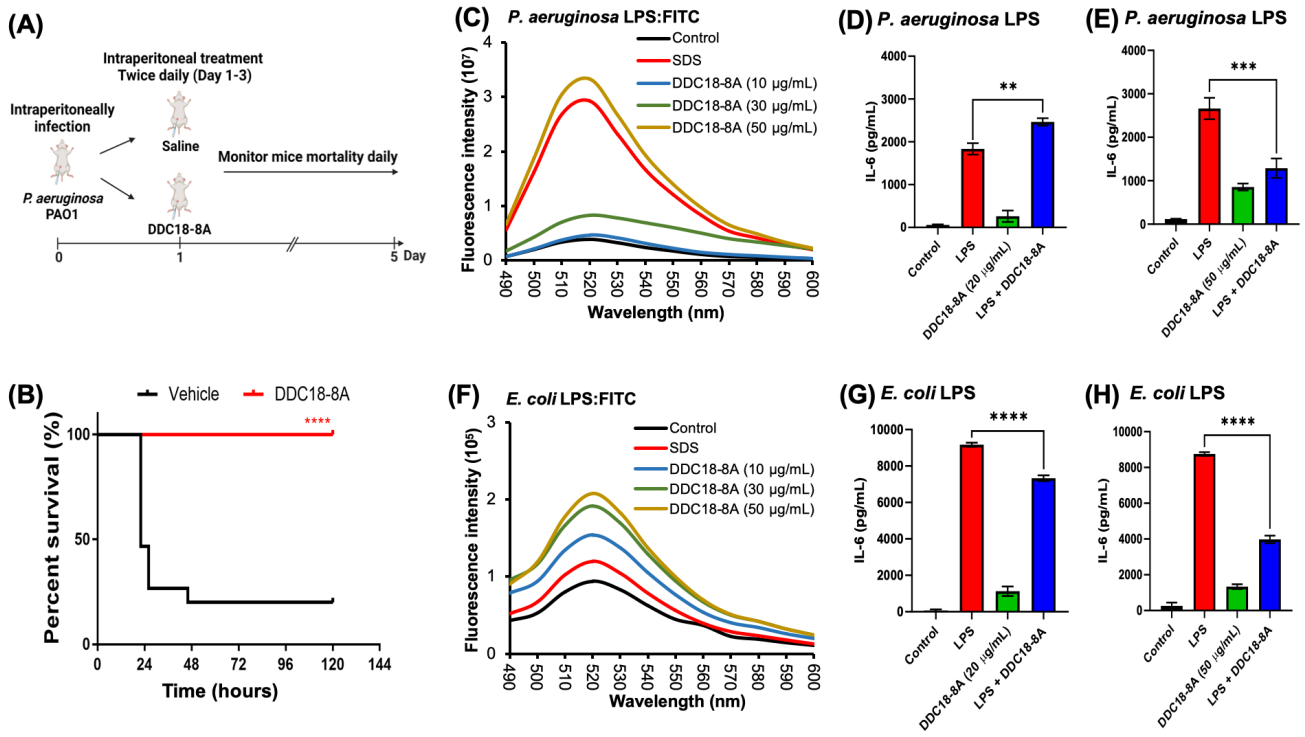

Figure 8. DDC18-8A attenuates bacteremia mediated mortality and dampens LPS-mediated proinflammatory response. (A) Experimental scheme of mouse bacteremia mortality study. (B) CD-1 mice (n = 15) were intraperitoneally-infected with 1.2 x 10^7 CFU of *P. aeruginosa* strain PAO1. Infected mice were treated intraperitoneally twice daily with either 5 mg/kg of DDC18-8A or an equivalent volume of sterile PBS, for 3 days. Mouse mortality was monitored for 120 hours. $^{****}p < 0.0001$ as determined by the Kaplan–Meier Log Rank Survival Test using GraphPad Prism (Version 9.0.2). (C) DDC18-8A interacts with LPS-FITC of *P. aeruginosa* in a dose dependent manner. SDS (2%) served a positive control. (D-E) DDC18-8A dampens the induction of IL-6 secretion in human peripheral blood monocytes (hPBMCs) by *P. aeruginosa* LPS in a concentration dependent manner. (F) DDC18-8A interacts with LPS-FITC of *E. coli* in a dose dependent manner. SDS (2%) served a positive control. (G-H) DDC18-8A dampens the induction of IL-6 secretion in hPBMCs by *E. coli* LPS in a concentration dependent manner. Error bars mean represent SD for n = 3 of a typical experiment performed independently three times. Statistical significance was determined using an unpaired two-tailed Student's t-test for the analysis of two groups and expressed as $^{**}p \leq 0.01$, $^{***}p \leq 0.001$, and $^{****}p \leq 0.0001$.

Among the virulence factors expressed by Gram-negative pathogens, lipopolysaccharides (LPS) potently stimulates proinflammatory cascade which may spiral out of control, leading to sepsis and endotoxic septic shock with a high burden of multi-organ organ failure and morbidity and mortality.[42-44] LPS forms aggregate and triggers excessive Toll receptor mediated immune response that lead to sepsis.[45-49] Unfortunately, effective therapy is not available and antibiotics remain the drugs of choice for sepsis.[50] Dysregulated hyperinflammation mediated by an increased production of proinflammatory cytokines such as IL-6 from macrophages and monocytes causes multiorgan failure.[50-51] Because the

DDC18-8A is amphiphilic and composed of a long hydrophobic alkyl chain and a small hydrophilic poly(amidoamine) dendron bearing amine terminals, we were curious whether it might interact with the amphipathic LPS on the outer membrane of Gram-negative bacteria. Several prior studies have reported AMPs and their derivatives can interact and disperse LPS aggregates and subsequently prevent excessive proinflammatory response.[52-54] If DDC18-8A interacts with LPS, it might attenuate proinflammatory responses and ultimately, sepsis pathogenesis. LPS is capable of self-assembling into aggregates, and because of aggregation, the fluorescence of FITC in the FITC-LPS is quenched. In contrast, dissociation of the aggregates by DDC18-8A may increase in the fluorescence of FITC. We then examined whether DDC18-8A was able to interact with *P. aeruginosa* LPS conjugated to FITC. Similar to the amphiphilic sodium dodecyl sulfate (SDS),[54-56] DDC18-8A increased the intensity of the fluorescence by several orders of magnitude in comparison to control, suggesting that the dendrimer was able to dissociate the *P. aeruginosa* LPS aggregates (Figure 8C). Importantly, DDC18-8A attenuated the production of IL-6 in human peripheral blood monocytes (hPBMCs) induced by LPS from *P. aeruginosa* (Figure 8D-E). Similar results were obtained with *E. coli* LPS (Figure 8F-H). Interestingly, DDC18-8A by itself induced a small increase in the expression of IL-6 (Figures 8D, E, G, H). The mechanism behind this minimal induction is unknown but may reflect physical interaction between DDC18-8A nanomicelles with the hPBMC cell membrane that led to minor activation of TLR4 and downstream signaling. Also, DDC18-8A appeared to be more effective in attenuating IL-6 induction in hPBMCs by *E. coli* LPS when compared to *P. aeruginosa* LPS, which may reflect structural differences between the LPS from these bacteria that resulted in differing disaggregation activities (compare Figure 8C versus 8F). Collectively, various results in Figures 4-8 illustrate the strong potential of DDC18-8A as a superior alternative to antibiotics in combating infectious diseases caused by evermore challenging antibiotic recalcitrant ESKAPE pathogens and in mitigating bacterial LPS-mediated sepsis.

SUMMARY

According to the U.S. CDC, antibiotic resistance is amongst some of the most serious threats that complicate current medicine and major economic burdens worldwide. One potential alternative to antibiotics, as we have demonstrated above, is the application of amphiphilic dendrimers to mimic the antibacterial activity of AMPs. More specifically, the dendrimer DDC18-8A demonstrated promising antibacterial efficacy against selected *P. aeruginosa*, MRSA, and *K. pneumoniae*. DDC18-8A significantly reduced the bacterial burden in immunocompetent mouse models of acute pneumonia and bacteremia, and in immunosuppressed soft tissue infection by *P. aeruginosa* and MRSA; and improved the survival of mice during lethal bacteremia challenge by *P. aeruginosa*. Thanks to its excellent pharmacokinetic properties, including favorable stability and resistant to rapid degradation by host and bacterial proteases, and favorable biodistribution, DDC18-8A at even 10-fold lower concentrations attained similar levels of bacterial clearance when compared against pathogen-specific antibiotics. Additionally, DDC18-8A

showed an excellent safety profile, and did not induce drug resistance. Finally, DDC18-8A was able to disaggregate LPS and dampen the secretion of the proinflammatory cytokine IL-6 implicated in the pathogenesis of sepsis. Thus, our study support the potential of the amphiphilic dendrimer DDC18-8A as an efficient antibacterial against infections by antibiotic resistant bacteria, including in cases of bacterial sepsis.[57-59] Its antibacterial efficacy should be further explored in the high-risk *P. aeruginosa* XDR clones includes ST235, ST111, ST233, ST244, ST357, ST308, ST175, ST277, ST654 and ST298 threatening hospitals worldwide;[60] both hospital-acquired MRSA (HA-MRSA) as well as the community-acquired MRSA (CA-MRSA), the latter clones can invade community settings and infect people without predisposing risk factors and cause both skin and soft tissue infections and health care-associated infections;[61-64] and epidemic carbapenem-resistant *K. pneumoniae* clone ST258 (and its single-locus variants ST11 and ST340)[65] and hypervirulent strains belonging to the K1 and K2 capsular serotypes.[66-68] Additional studies should also expand DDC18-8A treatment on other critical-priority healthcare burden ESKAPEE pathogens such as carbapenem-resistance *A. baumannii,* 3rd-generation cephalosporin-resistant *E. coli* and vancomycin-resistant *E. faecium*,[69] and in animal models of bacterial sepsis.

METHODS

Reagents

All reagents were purchased from Millipore-Sigma-Aldrich (St. Louis, MO, USA) and Thermo Fisher Scientific (Waltham, MA, USA), unless otherwise noted.

Synthesis and characterization of DDC18-8A

The synthesis of amphiphilic dendrimer DDC18-8A was carried out according to the well-established protocol published in our group.[27, 70] DDC18-8A was resuspended in sterile H_2O to the desirable concentrations and vortex vigorously for 5 minutes before use. The structural integrity and purity of DDC18-8A was confirmed using NMR and HRMS analysis (Figures S1-S2). ^{1}H NMR (400 MHz, CD_3OD): δ 7.90 (s, 1H, CH), 4.35-4.39 (t, 2H, CH_2), 3.80 (s, 2H, CH_2), 3.22-3.25 (m, 28H, CH_2), 2.71-2.83 (m, 44H, CH_2), 2.54-2.57 (m, 12H, CH_2), 2.33-2.43 (m, 28H, CH_2), 1.87-1.92 (m, 2H, CH_2), 1.26-1.30 (m, 30H, CH_2), 0.88-0.89 (t, 3H, CH_3); IR (cm^{-1}): υ 1644.6; HRMS: calculated for $C_{91}H_{186}N_{32}O_{14}^{4+}$ $[M+4H]^{4+}$ 488.1208, found 488.1294.

Encapsulation of Cy7.5 into DDC18-8A for biodistribution study

For in vivo live imaging of DDC18-8A biostability and biodistribution, we encapsulated the hydrophobic Cy7.5 in the DDC18-8A nanomicelles using film dispersion method.[71] DDC18-8A and Cy7.5 were mixed in 3:0.1 w/w ratio in $CHCl_3$: MeOH mixed solvent (3:1 v/v) and then evaporated on rotary evaporator until clear film appeared after removal of organic solvents. The thin film was dispersed in PBS buffer and vortexed for 10 min or until a clear solution was obtained. This solution was filtered through 0.22 μM

sterile filter to remove any non-encapsulated Cy7.5. Fluorescence spectroscopic analysis was used to quantify encapsulated Cy7.5 in dendrimer nanomicelles using Ex: 788 nm and Em: 808 nm wavelengths. The encapsulation efficiency of Cy7.5 was found to be 92% as calculated below: encapsulation efficiency (%) = W_t/W_o × 100%, with W_t represents the amount of Cy7.5 that loaded into nanoparticles; W_o represents the initial amount of Cy7.5 fed. The fluorescence emission spectrum of Cy7.5/DDC18-8A in water is provided in the Figure S3.

Bacterial cultures and growth conditions

The wild-type *P. aeruginosa* strain PAO1 was originally provided by Professor Michael Vasil (University of Colorado), as we have previously published.[72-77] MRSA strain USA300 LAC was provided by Professor Jianjun Cheng of the University of Illinois at Urbana-Champaign as we have published.[30] *K. pneumoniae* strain BAA1705 was as previously published.[31] Aliquots of the bacteria were cultured from frozen stocks in fresh lysogeny broth (LB) to desirable growth phase and diluted cell density for each assay. The OD at 600 nm was determined using a spectrophotometer and correlated with numbers of colony forming unit (CFU) after serial dilution plating on LB agar.

In vitro killing assays

In vitro bacterial killings were performed as previously described in PBS.[30, 32, 78] Overnight cultures of *P. aeruginosa* strain PAO1*,* MRSA USA300LAC*, and K. pneumoniae* BAA1705 were washed with sterile PBS and serially diluted to about approximately $10^{7\text{-}8}$ CFU mL^{-1}. The washed bacteria were resuspended in PBS and transferred to glass test tubes and received the indicated concentrations of DDC18-8A (pre-vortexed for 5 minutes) or equal volume of sterile H_2O, for the indicated duration. Daptomycin-mediated killing was performed with the supplementation of 0.5 mM $CaCl_2$ and 0.15 mM $MgCl_2$. The test tubes were rotated on a TC-7 rotary drum at speed setting 6 at 37° C. After incubation, bacterial killing was determined by serial dilution plating onto LB agar. All bacterial killing were performed independently three times in triplicate.

MIC and MBC determination

MIC values were determined as previous published.[79] Briefly, DDC18-8A were serially two-fold diluted in LB broth and mixed with an equal volume of bacterial suspensions in LB containing 1.0 × 10^6 CFU mL^{-1} bacteria in a clear and sterile 96-well microtiter plate (Thermo Scientific). After static incubation at 37°C for 18 hours, inhibition of bacterial growth were determined by OD_{600} measurements. The MICs were defined as the lowest concentrations of DDC18-8A with no visible growth of bacteria. MBC values were determined in the same manner, but with the additional CFU plating on the LB agar to confirm the minimal concentration of DDC18-8A that killed all bacteria completely.

Evolution of resistance

Resistance development assay was performed on *P. aeruginosa* strain PAO1 with DDC18-8A (MIC 12 ug mL^{-1}, Table 1) or tobramycin (MIC 1 μg mL^{-1}) as described previously.[80] Exponentially phase *P. aeruginosa* were diluted 1:100 in 1.0 mL LB in 2 mL microfuge tubes containing 0.25, 0.50, 1.0, 2.0, 4.0 x MIC of DDC18-8A or tobramycin (MIC as the control. Bacteria were incubated at 37°C, 225 rpm and passaged every 24-hour cycle. Bacterial culture from the highest concentration that allowed growth was diluted 1:100 into the fresh LB with various concentrations (0.25, 0.50, 1.0, 2.0, 4.0 x MIC) of the respective drug. As the MIC values changed, concentrations of the respective drug were adjusted for next passaging. Serial passaging was reiterated for 30 days, and changes in the MIC values were measured by dividing the respective daily MICs by the MIC on Day 1.

PrestoBlue cytotoxicity studies

Mouse macrophages RAW264.7, mouse fibroblast NIH3T3 and Chinese hamster ovary cells CHO-K1 were seeded at 1.0×10^4 cells/well in 96-well plates and allowed to grow overnight. Cells were then treated with various concentration (1.69 – 217 μg mL^{-1}) of the DDC18-8A for 48 hours, followed by addition of 10 μL PrestoBlue reagent to each well containing 100 μL of blank, control, or treated cells, and further incubated for another 3 hours at 37 °C. The changes in cell viability were detected by using fluorescence spectroscopy (excitation 570 nm; emission 610 nm). The cell viability was expressed as a percentage relative to the untreated cells. All samples were performed in triplicate.

Ethical statement

Animal experiments were performed in strict accordance with the Guide for the Care and Use of Laboratory Animals of the National Institutes of Health. Animal protocol was thoroughly reviewed and approved by the Institutional Animal Care and Use Committee (IACUC) at the University of Illinois at Urbana-Champaign, under the protocol # 22051. CD-1 mice (6–week old, both males and females, body weight males 27-35 g; females 22-30 g, both sexes in the same group) were purchased from Charles River (Wilmington, MA, U.S.). All mice were acclimated for one week prior to experimentation. All mice were housed in positively ventilated microisolator cages with automatic recirculating water located in a room with laminar, high efficiency particulate-filtered air, with full access to food, water, and bedding. At the completion of experiments, mice were euthanized by overdosing with CO_2 followed by cervical dislocation.

Toxicity studies in mice

CD-1 mice (groups of 5 males) were intraperitoneally injected twice daily with 5 mg/kg DDC18-8A or sterile saline control (in 50 μl) for seven days. Mice were weighed daily and euthanized on the 8th day. Blood was collected for biochemistry and complete blood count with differential analysis at the University

of Illinois at Urbana-Champaign Veterinary Diagnostic Laboratory, and compared to established reference range,[81] as well as based on the technical data provided by the Charles River Laboratories where the mice originated (https://www.criver.com/products-services/find-model/cd-1r-igs-mouse?region=3611). Major organs, including livers, lungs, kidneys, hearts and spleens were embedded in paraffin, sectioned, and stained with hematoxylin and eosin, and imaged using an Olympus DP70 light microscope (Olympus, Central Valley, PA, USA).

Pharmacokinetic analysis

For the *in vivo* live imaging of the DDC18-8A biostability and biodistribution, CD-1 mice (7–week old, male, groups of 3) were anesthetized with 3% isoflurane in an induction chamber. Mice received 1.67 mg/kg intraperitoneal injection with Cyanine7.5-labeled DDC18-8A (Cy7.5/DDC18-8A) imaged using an IVIS SpectrumCT Imaging system (PerkinElmer, Waltham, Massachusetts, USA). The following settings were used: binning factor = 1, f number = 1, field of view = 25.4, and fluorescence exposure time for 60 s. Images were analyzed by Living Image® Software (PerkinElmer).

Mouse model of acute pneumonia and bacteremia

For acute pneumonia, CD-1 mice (n = 8/group, males and females) were intranasally-inoculated with *P. aeruginosa* strain PAO1, MRSA strain USA300LAC, or *K. pneumoniae* strain BAA1705, respectively. For bacteremia, CD-1 mice (n = 6/group) were intraperitoneally-infected with the aforementioned bacterial strains. Infected mice were treated twice daily with intraperitoneally injection of 5 mg/kg of DDC18-8A. The control groups were treated with the same volume of sterile PBS or bacterial-specific antibiotic (PA01, tobramycin; USA300LAC, daptomycin; SQ, BAA1705, tigecycline). For acute pneumonia, lungs were harvested and processed at 48-hour post infection (hpi). For bacteremia, spleens and other organs (kidneys, hearts, lungs, livers) were analyzed at 24-hpi. Mouse tissues were homogenized in 1 mL sterile PBS using an Omni Soft Tissue Tip™ Homogenizer (Genizer LLC, Irvine, CA, USA). Bacterial burden was determined through serial dilution plating of the homogenate onto LB agar plates.

Immunosuppressed soft tissue infection studies

Seven–week old CD-1 mice (males and females) were rendered immunosuppressed (neutropenic) by intraperitoneal injections of cyclophosphamide (150 mg/kg) for four days from Day -5 to Day -1, as we and others have previously published.[32, 82-83] On the day prior to bacterial challenge, mice were anesthetized with intraperitoneal injection of ketamine (80-100 mg/kg) and xylazine (10-12.5 mg/kg), and fur on the right hind thigh region was removed by clipping with scissors, preceded by depilating gel administration. On Day 1, mice were anesthetized with isoflurane and inoculated intramuscularly with 20 μL of *P. aeruginosa* strain PAO1 and MRSA strain USA300 LAC, respectively, into the bicep femoris (thigh) with a 30 G needle. Infected mice were treated with either DDC18-8A, bacterial-specific antibiotic

(daptomycin for USA300LAC; tobramycin for PA01), or sterile PBS control. Bacterial burden in the thigh was determined at 48-hpi.

Mouse model of lethal bacteremic peritonitis

Mice were anesthetized with isoflurane and intraperitoneally-infected with *P. aeruginosa* strain PAO1. Mice were treated intraperitoneally twice daily with 5 mg/kg DDC18-8A for three days. Control group was administered sterile PBS for the same duration. Mouse mortality was monitored for 120 hours.

LPS disaggregation assay and interleukin (IL)-6 measurement

Binding and disaggregation of FITC-conjugated *E. coli* and *P. aeruginosa* LPS were performed as previously published.[53] *E. coli* FITC-LPS was commercially sourced (MilliporeSigma #F3665). *P. aeruginosa* LPS (MilliporeSigma #L9143) was conjugated to FITC as previously published.[84] For IL-6 assay, human PBMCs (Lonza #CC-2705, Hayward, CA, USA). PBMCs were exposed to *E. coli* or *P. aeruginosa* FITC-LPS as described.[53] IL-6 levels in the PBMCs culture supernatant was measured by using the human ELISA kit (BD Biosciences, San Jose, CA, USA) following the manufacturer's instructions.

Statistical analysis

Quantitative data was expressed as the mean ± standard deviation, and was calculated using their respective functions. Statistical significance was determined by using the Student's t-test. We used an unpaired two-tailed Student's t-test for the analysis of two groups. Statistical significance was expressed as $*p \leq 0.05$, $**p \leq 0.01$, $***p \leq 0.001$, $****p \leq 0.001$, or ns (not significant). For survival analyses, a Kaplan-Meier Log Rank Survival Test was performed using the GraphPad Prism Version 9.0.2 Software.

Author contributions

NK, DD, SQL, LP and GWL conceived, designed and conducted experiments, acquired data, analyzed data, and wrote the manuscript. SHK, CG, MWO, SYC, NZ, ZH conducted experiments, acquired data, analyzed data, and reviewed the manuscript. LTOL reviewed the manuscript.

Disclosure statement

The authors have no conflict in financial interests and are solely responsible for experimental designs and data analysis. The funders had no role in study design, data collection and interpretation, or the decision to submit the work for publication.

Acknowledgements

We thank Professors Michael Vasil (University of Colorado Health Science Center) for the *P. aeruginosa* strain PAO1 and Jianjun Cheng (University of Illinois at Urbana-Champaign) for MRSA strain USA300 LAC. This work was partly supported by the NIH grant (HL142626) to GWL, a joint seed grant by the Hebrew University of Jerusalem and the University of Illinois to ZH and G.W.L., and the French National Research Agency under the frame of the Era-Net EURONANOMED European Research projects 'TABRAINFEC' and 'antineuropatho' to LP.

REFERENCES

1. CDC *Antibiotic Resistance Threats in the United States, 2019*; U.S. Department of Health and Human Services, CDC: Atlanta, GA, 2019.
2. Stone, P. W., Economic burden of healthcare-associated infections: an American perspective. *Expert Rev Pharmacoecon Outcomes Res* **2009,** *9* (5), 417-22. DOI: 10.1586/erp.09.53.
3. Magiorakos, A. P.; Srinivasan, A.; Carey, R. B.; Carmeli, Y.; Falagas, M. E.; Giske, C. G.; Harbarth, S.; Hindler, J. F.; Kahlmeter, G.; Olsson-Liljequist, B.; Paterson, D. L.; Rice, L. B.; Stelling, J.; Struelens, M. J.; Vatopoulos, A.; Weber, J. T.; Monnet, D. L., Multidrug-resistant, extensively drug-resistant and pandrug-resistant bacteria: an international expert proposal for interim standard definitions for acquired resistance. *Clin Microbiol Infect* **2012,** *18* (3), 268-81. DOI: 10.1111/j.1469-0691.2011.03570.x.
4. D'Costa, V. M.; McGrann, K. M.; Hughes, D. W.; Wright, G. D., Sampling the antibiotic resistome. *Science* **2006,** *311* (5759), 374-7. DOI: 10.1126/science.1120800.
5. Gaze, W. H.; Krone, S. M.; Larsson, D. G.; Li, X. Z.; Robinson, J. A.; Simonet, P.; Smalla, K.; Timinouni, M.; Topp, E.; Wellington, E. M.; Wright, G. D.; Zhu, Y. G., Influence of humans on evolution and mobilization of environmental antibiotic resistome. *Emerg Infect Dis* **2013,** *19* (7). DOI: 10.3201/eid1907.120871.
6. Barbier, F.; Andremont, A.; Wolff, M.; Bouadma, L., Hospital-acquired pneumonia and ventilator-associated pneumonia: recent advances in epidemiology and management. *Curr Opin Pulm Med* **2013,** *19* (3), 216-28. DOI: 10.1097/MCP.0b013e32835f27be.
7. Jean, S. S.; Chang, Y. C.; Lin, W. C.; Lee, W. S.; Hsueh, P. R.; Hsu, C. W., Epidemiology, Treatment, and Prevention of Nosocomial Bacterial Pneumonia. *J Clin Med* **2020,** *9* (1). DOI: 10.3390/jcm9010275.
8. Döring, G.; Parameswaran, I. G.; Murphy, T. F., Differential adaptation of microbial pathogens to airways of patients with cystic fibrosis and chronic obstructive pulmonary disease. *FEMS Microbiol Rev* **2011,** *35* (1), 124-46. DOI: 10.1111/j.1574-6976.2010.00237.x.
9. Riquelme, S. A.; Ahn, D.; Prince, A., Pseudomonas aeruginosa and Klebsiella pneumoniae Adaptation to Innate Immune Clearance Mechanisms in the Lung. *J Innate Immun* **2018,** *10* (5-6), 442-454. DOI: 10.1159/000487515.
10. Mittal, R.; Lisi, C. V.; Gerring, R.; Mittal, J.; Mathee, K.; Narasimhan, G.; Azad, R. K.; Yao, Q.; Grati, M.; Yan, D.; Eshraghi, A. A.; Angeli, S. I.; Telischi, F. F.; Liu, X. Z., Current concepts in the pathogenesis and treatment of chronic suppurative otitis media. *J Med Microbiol* **2015,** *64* (10), 1103-1116. DOI: 10.1099/jmm.0.000155.
11. Fleiszig, S. M. J.; Kroken, A. R.; Nieto, V.; Grosser, M. R.; Wan, S. J.; Metruccio, M. M. E.; Evans, D. J., Contact lens-related corneal infection: Intrinsic resistance and its compromise. *Prog Retin Eye Res* **2020,** *76*, 100804. DOI: 10.1016/j.preteyeres.2019.100804.
12. Hilliam, Y.; Kaye, S.; Winstanley, C., and microbial keratitis. *J Med Microbiol* **2020,** *69* (1), 3-13. DOI: 10.1099/jmm.0.001110.
13. Shupp, J. W.; Pavlovich, A. R.; Jeng, J. C.; Pezzullo, J. C.; Oetgen, W. J.; Jaskille, A. D.; Jordan, M. H.; Shoham, S., Epidemiology of bloodstream infections in burn-injured patients: a review of the national burn repository. *J Burn Care Res* **2010,** *31* (4), 521-8. DOI: 10.1097/BCR.0b013e3181e4d5e7.

14. Estrada, S.; Lodise, T. P.; Tillotson, G. S.; Delaportas, D., The Real-World Economic and Clinical Management of Adult Patients with Skin and Soft Tissue Infections (SSTIs) with Oritavancin: Data from Two Multicenter Observational Cohort Studies. *Drugs Real World Outcomes* **2020,** *7* (Suppl 1), 6-12. DOI: 10.1007/s40801-020-00199-3.
15. Restuccia, P. A.; Cunha, B. A., Klebsiella. *Infect Control* **1984,** *5* (7), 343-7. DOI: 10.1017/s0195941700060549.
16. Magill, S. S.; O'Leary, E.; Janelle, S. J.; Thompson, D. L.; Dumyati, G.; Nadle, J.; Wilson, L. E.; Kainer, M. A.; Lynfield, R.; Greissman, S.; Ray, S. M.; Beldavs, Z.; Gross, C.; Bamberg, W.; Sievers, M.; Concannon, C.; Buhr, N.; Warnke, L.; Maloney, M.; Ocampo, V.; Brooks, J.; Oyewumi, T.; Sharmin, S.; Richards, K.; Rainbow, J.; Samper, M.; Hancock, E. B.; Leaptrot, D.; Scalise, E.; Badrun, F.; Phelps, R.; Edwards, J. R.; Emerging Infections Program Hospital Prevalence Survey, T., Changes in Prevalence of Health Care-Associated Infections in U.S. Hospitals. *N Engl J Med* **2018,** *379* (18), 1732-1744. DOI: 10.1056/NEJMoa1801550.
17. Choby, J. E.; Howard-Anderson, J.; Weiss, D. S., Hypervirulent Klebsiella pneumoniae - clinical and molecular perspectives. *J Intern Med* **2020,** *287* (3), 283-300. DOI: 10.1111/joim.13007.
18. Pomakova, D. K.; Hsiao, C. B.; Beanan, J. M.; Olson, R.; MacDonald, U.; Keynan, Y.; Russo, T. A., Clinical and phenotypic differences between classic and hypervirulent Klebsiella pneumonia: an emerging and under-recognized pathogenic variant. *Eur J Clin Microbiol Infect Dis* **2012,** *31* (6), 981-9. DOI: 10.1007/s10096-011-1396-6.
19. Russo, T. A.; Marr, C. M., Hypervirulent Klebsiella pneumoniae. *Clin Microbiol Rev* **2019,** *32* (3). DOI: 10.1128/CMR.00001-19.
20. Fjell, C. D.; Hiss, J. A.; Hancock, R. E.; Schneider, G., Designing antimicrobial peptides: form follows function. *Nat Rev Drug Discov* **2011,** *11* (1), 37-51. DOI: 10.1038/nrd3591.
21. Lyu, Z.; Yang, P.; Lei, J.; Zhao, J., Biological Function of Antimicrobial Peptides on Suppressing Pathogens and Improving Host Immunity. *Antibiotics (Basel)* **2023,** *12* (6). DOI: 10.3390/antibiotics12061037.
22. Mookherjee, N.; Anderson, M. A.; Haagsman, H. P.; Davidson, D. J., Antimicrobial host defence peptides: functions and clinical potential. *Nat Rev Drug Discov* **2020,** *19* (5), 311-332. DOI: 10.1038/s41573-019-0058-8.
23. Galanakou, C.; Dhumal, D.; Peng, L., Amphiphilic dendrimers against antibiotic resistance: light at the end of the tunnel? *Biomater Sci* **2023,** *11* (10), 3379-3393. DOI: 10.1039/d2bm01878k.
24. Lai, Z.; Jian, Q.; Li, G.; Shao, C.; Zhu, Y.; Yuan, X.; Chen, H.; Shan, A., Self-Assembling Peptide Dendron Nanoparticles with High Stability and a Multimodal Antimicrobial Mechanism of Action. *ACS Nano* **2021,** *15* (10), 15824-15840. DOI: 10.1021/acsnano.1c03301.
25. Siriwardena, T. N.; Stach, M.; He, R.; Gan, B. H.; Javor, S.; Heitz, M.; Ma, L.; Cai, X.; Chen, P.; Wei, D.; Li, H.; Ma, J.; Kohler, T.; van Delden, C.; Darbre, T.; Reymond, J. L., Lipidated Peptide Dendrimers Killing Multidrug-Resistant Bacteria. *J Am Chem Soc* **2018,** *140* (1), 423-432. DOI: 10.1021/jacs.7b11037.
26. Sowinska, M.; Laskowska, A.; Guspiel, A.; Solecka, J.; Bochynska-Czyz, M.; Lipkowski, A. W.; Trzeciak, K.; Urbanczyk-Lipkowska, Z., Bioinspired Amphiphilic Peptide Dendrimers as Specific and Effective Compounds against Drug Resistant Clinical Isolates of E. coli. *Bioconjug Chem* **2018,** *29* (11), 3571-3585. DOI: 10.1021/acs.bioconjchem.8b00544.
27. Dhumal, D.; Maron, B.; Malach, E.; Lyu, Z.; Ding, L.; Marson, D.; Laurini, E.; Tintaru, A.; Ralahy, B.; Giorgio, S.; Pricl, S.; Hayouka, Z.; Peng, L., Dynamic self-assembling supramolecular dendrimer nanosystems as potent antibacterial candidates against drug-resistant bacteria and biofilms. *Nanoscale* **2022,** *14* (26), 9286-9296. DOI: 10.1039/d2nr02305a.
28. Mintzer, M. A.; Dane, E. L.; O'Toole, G. A.; Grinstaff, M. W., Exploiting dendrimer multivalency to combat emerging and re-emerging infectious diseases. *Mol Pharm* **2012,** *9* (3), 342-54. DOI: 10.1021/mp2005033.
29. Zhou, Z.; Cong, M.; Li, M.; Tintaru, A.; Li, J.; Yao, J.; Xia, Y.; Peng, L., Negative dendritic effect on enzymatic hydrolysis of dendrimer conjugates. *Chem Commun (Camb)* **2018,** *54* (47), 5956-5959. DOI: 10.1039/c8cc01221k.
30. Bennett, R. C.; Oh, M. W.; Kuo, S. H.; Belo, Y.; Maron, B.; Malach, E.; Lin, J.; Hayouka, Z.; Lau, G. W., Random Peptide Mixtures as Safe and Effective Antimicrobials against Pseudomonas aeruginosa and MRSA in Mouse Models of Bacteremia and Pneumonia. *ACS Infect Dis* **2021,** *7* (3), 672-680. DOI: 10.1021/acsinfecdis.0c00871.

31. Parker, E. N.; Drown, B. S.; Geddes, E. J.; Lee, H. Y.; Ismail, N.; Lau, G. W.; Hergenrother, P. J., Implementation of permeation rules leads to a FabI inhibitor with activity against Gram-negative pathogens. *Nat Microbiol* **2020,** *5* (1), 67-75. DOI: 10.1038/s41564-019-0604-5.
32. Caraway, H. E.; Lau, J. Z.; Maron, B.; Oh, M. W.; Belo, Y.; Brill, A.; Malach, E.; Ismail, N.; Hayouka, Z.; Lau, G. W., Antimicrobial Random Peptide Mixtures Eradicate Acinetobacter baumannii Biofilms and Inhibit Mouse Models of Infection. *Antibiotics (Basel)* **2022,** *11* (3). DOI: 10.3390/antibiotics11030413.
33. Meylan, S.; Porter, C. B. M.; Yang, J. H.; Belenky, P.; Gutierrez, A.; Lobritz, M. A.; Park, J.; Kim, S. H.; Moskowitz, S. M.; Collins, J. J., Carbon Sources Tune Antibiotic Susceptibility in Pseudomonas aeruginosa via Tricarboxylic Acid Cycle Control. *Cell Chem Biol* **2017,** *24* (2), 195-206. DOI: 10.1016/j.chembiol.2016.12.015.
34. Choi, S.; Moon, S. M.; Park, S. J.; Lee, S. C.; Jung, K. H.; Sung, H. S.; Kim, M. N.; Jung, J.; Kim, M. J.; Kim, S. H.; Lee, S. O.; Choi, S. H.; Jeong, J. Y.; Woo, J. H.; Kim, Y. S.; Chong, Y. P., Antagonistic Effect of Colistin on Vancomycin Activity against Methicillin-Resistant Staphylococcus aureus in In Vitro and In Vivo Studies. *Antimicrob Agents Chemother* **2020,** *64* (4). DOI: 10.1128/AAC.01925-19.
35. Lou, W.; Venkataraman, S.; Zhong, G.; Ding, B.; Tan, J. P. K.; Xu, L.; Fan, W.; Yang, Y. Y., Antimicrobial polymers as therapeutics for treatment of multidrug-resistant Klebsiella pneumoniae lung infection. *Acta Biomater* **2018,** *78*, 78-88. DOI: 10.1016/j.actbio.2018.07.038.
36. Azzopardi, E. A.; Ferguson, E. L.; Thomas, D. W., The enhanced permeability retention effect: a new paradigm for drug targeting in infection. *J Antimicrob Chemother* **2013,** *68* (2), 257-74. DOI: 10.1093/jac/dks379.
37. Maeda, H.; Wu, J.; Sawa, T.; Matsumura, Y.; Hori, K., Tumor vascular permeability and the EPR effect in macromolecular therapeutics: a review. *J Control Release* **2000,** *65* (1-2), 271-84. DOI: 10.1016/s0168-3659(99)00248-5.
38. Matsumura, Y.; Maeda, H., A new concept for macromolecular therapeutics in cancer chemotherapy: mechanism of tumoritropic accumulation of proteins and the antitumor agent smancs. *Cancer Res* **1986,** *46* (12 Pt 1), 6387-92.
39. Garcia Chavez, M.; Garcia, A.; Lee, H. Y.; Lau, G. W.; Parker, E. N.; Komnick, K. E.; Hergenrother, P. J., Synthesis of Fusidic Acid Derivatives Yields a Potent Antibiotic with an Improved Resistance Profile. *ACS Infect Dis* **2021,** *7* (2), 493-505. DOI: 10.1021/acsinfecdis.0c00869.
40. Boylan, C. J.; Campanale, K.; Iversen, P. W.; Phillips, D. L.; Zeckel, M. L.; Parr, T. R., Pharmacodynamics of oritavancin (LY333328) in a neutropenic-mouse thigh model of Staphylococcus aureus infection. *Antimicrob Agents Chemother* **2003,** *47* (5), 1700-6. DOI: 10.1128/aac.47.5.1700-1706.2003.
41. Cheah, S. E.; Wang, J.; Nguyen, V. T.; Turnidge, J. D.; Li, J.; Nation, R. L., New pharmacokinetic/pharmacodynamic studies of systemically administered colistin against Pseudomonas aeruginosa and Acinetobacter baumannii in mouse thigh and lung infection models: smaller response in lung infection. *J Antimicrob Chemother* **2015,** *70* (12), 3291-7. DOI: 10.1093/jac/dkv267.
42. Daniel, M.; Bedoui, Y.; Vagner, D.; Raffray, L.; Ah-Pine, F.; Doray, B.; Gasque, P., Pathophysiology of Sepsis and Genesis of Septic Shock: The Critical Role of Mesenchymal Stem Cells (MSCs). *Int J Mol Sci* **2022,** *23* (16). DOI: 10.3390/ijms23169274.
43. Foster, D. M.; Kellum, J. A., Endotoxic Septic Shock: Diagnosis and Treatment. *Int J Mol Sci* **2023,** *24* (22). DOI: 10.3390/ijms242216185.
44. Wang, M.; Feng, J.; Zhou, D.; Wang, J., Bacterial lipopolysaccharide-induced endothelial activation and dysfunction: a new predictive and therapeutic paradigm for sepsis. *Eur J Med Res* **2023,** *28* (1), 339. DOI: 10.1186/s40001-023-01301-5.
45. Aderem, A.; Ulevitch, R. J., Toll-like receptors in the induction of the innate immune response. *Nature* **2000,** *406* (6797), 782-7. DOI: 10.1038/35021228.
46. Cohen, J., The immunopathogenesis of sepsis. *Nature* **2002,** *420* (6917), 885-91. DOI: 10.1038/nature01326.
47. Shahkar, L.; Keshtkar, A.; Mirfazeli, A.; Ahani, A.; Roshandel, G., The role of IL-6 for predicting neonatal sepsis: a systematic review and meta-analysis. *Iran J Pediatr* **2011,** *21* (4), 411-7.
48. Hou, T.; Huang, D.; Zeng, R.; Ye, Z.; Zhang, Y., Accuracy of serum interleukin (IL)-6 in sepsis diagnosis: a systematic review and meta-analysis. *Int J Clin Exp Med* **2015,** *8* (9), 15238-45.

49. Ferdosian, F.; Jarahzadeh, M. H.; Bahrami, R.; Nafei, Z.; Jafari, M.; Raee-Ezzabadi, A.; Mirjalili, S. R.; Neamatzadeh, H., Association of IL-6 -174G > C Polymorphism with Susceptibility to Childhood Sepsis: A Systematic Review and Meta-Analysis. *Fetal Pediatr Pathol* **2021,** *40* (6), 638-652. DOI: 10.1080/15513815.2020.1723149.
50. Uppu, D. S.; Ghosh, C.; Haldar, J., Surviving sepsis in the era of antibiotic resistance: are there any alternative approaches to antibiotic therapy? *Microb Pathog* **2015,** *80*, 7-13. DOI: 10.1016/j.micpath.2015.02.001.
51. Hancock, R. E.; Nijnik, A.; Philpott, D. J., Modulating immunity as a therapy for bacterial infections. *Nat Rev Microbiol* **2012,** *10* (4), 243-54. DOI: 10.1038/nrmicro2745.
52. Bowdish, D. M.; Davidson, D. J.; Lau, Y. E.; Lee, K.; Scott, M. G.; Hancock, R. E., Impact of LL-37 on anti-infective immunity. *J Leukoc Biol* **2005,** *77* (4), 451-9. DOI: 10.1189/jlb.0704380.
53. Uppu, D. S.; Haldar, J., Lipopolysaccharide Neutralization by Cationic-Amphiphilic Polymers through Pseudoaggregate Formation. *Biomacromolecules* **2016,** *17* (3), 862-73. DOI: 10.1021/acs.biomac.5b01567.
54. Ghosh, C.; Harmouche, N.; Bechinger, B.; Haldar, J., Aryl-Alkyl-Lysines Interact with Anionic Lipid Components of Bacterial Cell Envelope Eliciting Anti-Inflammatory and Antibiofilm Properties. *ACS Omega* **2018,** *3* (8), 9182-9190. DOI: 10.1021/acsomega.8b01052.
55. Rosenfeld, Y.; Lev, N.; Shai, Y., Effect of the hydrophobicity to net positive charge ratio on antibacterial and anti-endotoxin activities of structurally similar antimicrobial peptides. *Biochemistry* **2010,** *49* (5), 853-61. DOI: 10.1021/bi900724x.
56. Ong, Z. Y.; Cheng, J.; Huang, Y.; Xu, K.; Ji, Z.; Fan, W.; Yang, Y. Y., Effect of stereochemistry, chain length and sequence pattern on antimicrobial properties of short synthetic beta-sheet forming peptide amphiphiles. *Biomaterials* **2014,** *35* (4), 1315-25. DOI: 10.1016/j.biomaterials.2013.10.053.
57. Polcyn, P.; Jurczak, M.; Rajnisz, A.; Solecka, J.; Urbanczyk-Lipkowska, Z., Design of antimicrobially active small amphiphilic peptide dendrimers. *Molecules* **2009,** *14* (10), 3881-905. DOI: 10.3390/molecules14103881.
58. Namata, F.; Sanz Del Olmo, N.; Molina, N.; Malkoch, M., Synthesis and Characterization of Amino-Functional Polyester Dendrimers Based On Bis-MPA with Enhanced Hydrolytic Stability and Inherent Antibacterial Properties. *Biomacromolecules* **2023,** *24* (2), 858-867. DOI: 10.1021/acs.biomac.2c01286.
59. Jafari, P.; Luscher, A.; Siriwardena, T.; Michetti, M.; Que, Y. A.; Rahme, L. G.; Reymond, J. L.; Raffoul, W.; Van Delden, C.; Applegate, L. A.; Kohler, T., Antimicrobial Peptide Dendrimers and Quorum-Sensing Inhibitors in Formulating Next-Generation Anti-Infection Cell Therapy Dressings for Burns. *Molecules* **2021,** *26* (13). DOI: 10.3390/molecules26133839.
60. Del Barrio-Tofino, E.; Lopez-Causape, C.; Oliver, A., Pseudomonas aeruginosa epidemic high-risk clones and their association with horizontally-acquired beta-lactamases: 2020 update. *Int J Antimicrob Agents* **2020,** *56* (6), 106196. DOI: 10.1016/j.ijantimicag.2020.106196.
61. Elston, D. M., Status update: hospital-acquired and community-acquired methicillin-resistant Staphylococcus aureus. *Cutis* **2007,** *79* (6 Suppl), 37-42.
62. Levine, D. P.; Cushing, R. D.; Jui, J.; Brown, W. J., Community-acquired methicillin-resistant Staphylococcus aureus endocarditis in the Detroit Medical Center. *Ann Intern Med* **1982,** *97* (3), 330-8. DOI: 10.7326/0003-4819-97-3-330.
63. Saravolatz, L. D.; Pohlod, D. J.; Arking, L. M., Community-acquired methicillin-resistant Staphylococcus aureus infections: a new source for nosocomial outbreaks. *Ann Intern Med* **1982,** *97* (3), 325-9. DOI: 10.7326/0003-4819-97-3-325.
64. Otter, J. A.; French, G. L., Community-associated meticillin-resistant Staphylococcus aureus strains as a cause of healthcare-associated infection. *J Hosp Infect* **2011,** *79* (3), 189-93. DOI: 10.1016/j.jhin.2011.04.028.
65. Chen, L.; Mathema, B.; Chavda, K. D.; DeLeo, F. R.; Bonomo, R. A.; Kreiswirth, B. N., Carbapenemase-producing Klebsiella pneumoniae: molecular and genetic decoding. *Trends Microbiol* **2014,** *22* (12), 686-96. DOI: 10.1016/j.tim.2014.09.003.
66. Siu, L. K.; Yeh, K. M.; Lin, J. C.; Fung, C. P.; Chang, F. Y., Klebsiella pneumoniae liver abscess: a new invasive syndrome. *Lancet Infect Dis* **2012,** *12* (11), 881-7. DOI: 10.1016/S1473-3099(12)70205-0.
67. Bialek-Davenet, S.; Criscuolo, A.; Ailloud, F.; Passet, V.; Jones, L.; Delannoy-Vieillard, A. S.; Garin, B.; Le Hello, S.; Arlet, G.; Nicolas-Chanoine, M. H.; Decre, D.; Brisse, S., Genomic definition of hypervirulent and multidrug-

resistant Klebsiella pneumoniae clonal groups. *Emerg Infect Dis* **2014,** *20* (11), 1812-20. DOI: 10.3201/eid2011.140206.
68. Brisse, S.; Fevre, C.; Passet, V.; Issenhuth-Jeanjean, S.; Tournebize, R.; Diancourt, L.; Grimont, P., Virulent clones of Klebsiella pneumoniae: identification and evolutionary scenario based on genomic and phenotypic characterization. *PloS one* **2009,** *4* (3), e4982. DOI: 10.1371/journal.pone.0004982.
69. Tacconelli, E.; Carrara, E.; Savoldi, A.; Harbarth, S.; Mendelson, M.; Monnet, D. L.; Pulcini, C.; Kahlmeter, G.; Kluytmans, J.; Carmeli, Y.; Ouellette, M.; Outterson, K.; Patel, J.; Cavaleri, M.; Cox, E. M.; Houchens, C. R.; Grayson, M. L.; Hansen, P.; Singh, N.; Theuretzbacher, U.; Magrini, N.; Group, W. H. O. P. P. L. W., Discovery, research, and development of new antibiotics: the WHO priority list of antibiotic-resistant bacteria and tuberculosis. *Lancet Infect Dis* **2018,** *18* (3), 318-327. DOI: 10.1016/S1473-3099(17)30753-3.
70. Yu, T.; Liu, X.; Bolcato-Bellemin, A. L.; Wang, Y.; Liu, C.; Erbacher, P.; Qu, F.; Rocchi, P.; Behr, J. P.; Peng, L., An amphiphilic dendrimer for effective delivery of small interfering RNA and gene silencing in vitro and in vivo. *Angew Chem Int Ed Engl* **2012,** *51* (34), 8478-84. DOI: 10.1002/anie.201203920.
71. Jiang, Y.; Lyu, Z.; Ralahy, B.; Liu, J.; Roussel, T.; Ding, L.; Tang, J.; Kosta, A.; Giorgio, S.; Tomasini, R.; Liang, X. J.; Dusetti, N.; Iovanna, J.; Peng, L., Dendrimer nanosystems for adaptive tumor-assisted drug delivery via extracellular vesicle hijacking. *Proc Natl Acad Sci U S A* **2023,** *120* (7), e2215308120. DOI: 10.1073/pnas.2215308120.
72. Holloway, B. W.; Krishnapillai, V.; Morgan, A. F., Chromosomal genetics of Pseudomonas. *Microbiol Rev* **1979,** *43* (1), 73-102. DOI: 10.1128/mr.43.1.73-102.1979.
73. Zhang, S.; Chen, Y.; Potvin, E.; Sanschagrin, F.; Levesque, R. C.; McCormack, F. X.; Lau, G. W., Comparative signature-tagged mutagenesis identifies Pseudomonas factors conferring resistance to the pulmonary collectin SP-A. *PLoS Pathog* **2005,** *1* (3), 259-68. DOI: 10.1371/journal.ppat.0010031.
74. Zhang, S.; McCormack, F. X.; Levesque, R. C.; O'Toole, G. A.; Lau, G. W., The flagellum of Pseudomonas aeruginosa is required for resistance to clearance by surfactant protein A. *PloS one* **2007,** *2* (6), e564. DOI: 10.1371/journal.pone.0000564.
75. Tan, R. M.; Kuang, Z.; Hao, Y.; Lee, F.; Lee, T.; Lee, R. J.; Lau, G. W., Type IV pilus glycosylation mediates resistance of Pseudomonas aeruginosa to opsonic activities of the pulmonary surfactant protein A. *Infect Immun* **2015,** *83* (4), 1339-46. DOI: 10.1128/iai.02874-14.
76. Kuang, Z.; Bennett, R. C.; Lin, J.; Hao, Y.; Zhu, L.; Akinbi, H. T.; Lau, G. W., Surfactant phospholipids act as molecular switches for premature induction of quorum sensing-dependent virulence in. *Virulence* **2020,** *11* (1), 1090-1107. DOI: 10.1080/21505594.2020.1809327.
77. Kuang, Z.; Hao, Y.; Hwang, S.; Zhang, S.; Kim, E.; Akinbi, H. T.; Schurr, M. J.; Irvin, R. T.; Hassett, D. J.; Lau, G. W., The Pseudomonas aeruginosa flagellum confers resistance to pulmonary surfactant protein-A by impacting the production of exoproteases through quorum-sensing. *Mol Microbiol* **2011,** *79* (5), 1220-35. DOI: 10.1111/j.1365-2958.2010.07516.x.
78. Lau, J. Z.; Kuo, S. H.; Belo, Y.; Malach, E.; Maron, B.; Caraway, H. E.; Oh, M. W.; Zhang, Y.; Ismail, N.; Lau, G. W.; Hayouka, Z., Antibacterial efficacy of an ultra-short palmitoylated random peptide mixture in mouse models of infection by carbapenem-resistant Klebsiella pneumoniae. *Antimicrob Agents Chemother* **2023,** *67* (11), e0057423. DOI: 10.1128/aac.00574-23.
79. Song, M.; Liu, Y.; Huang, X.; Ding, S.; Wang, Y.; Shen, J.; Zhu, K., A broad-spectrum antibiotic adjuvant reverses multidrug-resistant Gram-negative pathogens. *Nat Microbiol* **2020,** *5* (8), 1040-1050. DOI: 10.1038/s41564-020-0723-z.
80. Le, P.; Kunold, E.; Macsics, R.; Rox, K.; Jennings, M. C.; Ugur, I.; Reinecke, M.; Chaves-Moreno, D.; Hackl, M. W.; Fetzer, C.; Mandl, F. A. M.; Lehmann, J.; Korotkov, V. S.; Hacker, S. M.; Kuster, B.; Antes, I.; Pieper, D. H.; Rohde, M.; Wuest, W. M.; Medina, E.; Sieber, S. A., Repurposing human kinase inhibitors to create an antibiotic active against drug-resistant Staphylococcus aureus, persisters and biofilms. *Nat Chem* **2020,** *12* (2), 145-158. DOI: 10.1038/s41557-019-0378-7.
81. Serfilippi, L. M.; Pallman, D. R.; Russell, B., Serum clinical chemistry and hematology reference values in outbred stocks of albino mice from three commonly used vendors and two inbred strains of albino mice. *Contemp Top Lab Anim Sci* **2003,** *42* (3), 46-52.

82. Sabet, M.; Tarazi, Z.; Griffith, D. C., Activity of Meropenem-Vaborbactam against Pseudomonas aeruginosa and Acinetobacter baumannii in a Neutropenic Mouse Thigh Infection Model. *Antimicrob Agents Chemother* **2019,** *63* (1). DOI: 10.1128/aac.01665-18.
83. Sabet, M.; Tarazi, Z.; Griffith, D. C., Pharmacodynamics of Meropenem against Acinetobacter baumannii in a Neutropenic Mouse Thigh Infection Model. *Antimicrob Agents Chemother* **2020,** *64* (4). DOI: 10.1128/AAC.02388-19.
84. Troelstra, A.; Antal-Szalmas, P.; de Graaf-Miltenburg, L. A.; Weersink, A. J.; Verhoef, J.; Van Kessel, K. P.; Van Strijp, J. A., Saturable CD14-dependent binding of fluorescein-labeled lipopolysaccharide to human monocytes. *Infect Immun* **1997,** *65* (6), 2272-7. DOI: 10.1128/iai.65.6.2272-2277.1997.